AD-A080 223 CALIFORNIA UNIV BERKELEY DEPT OF MATERIALS SCIENCE A--ETC F/G 11/6
ADVANCES IN THE HEAT TREATMENT OF STEELS.(U)
JUL 79 J W MORRIS, J I KIM, C K SYN N00014-75-C-0154
UNCLASSIFIED TR-9 NL

| OF |
AD
A080223

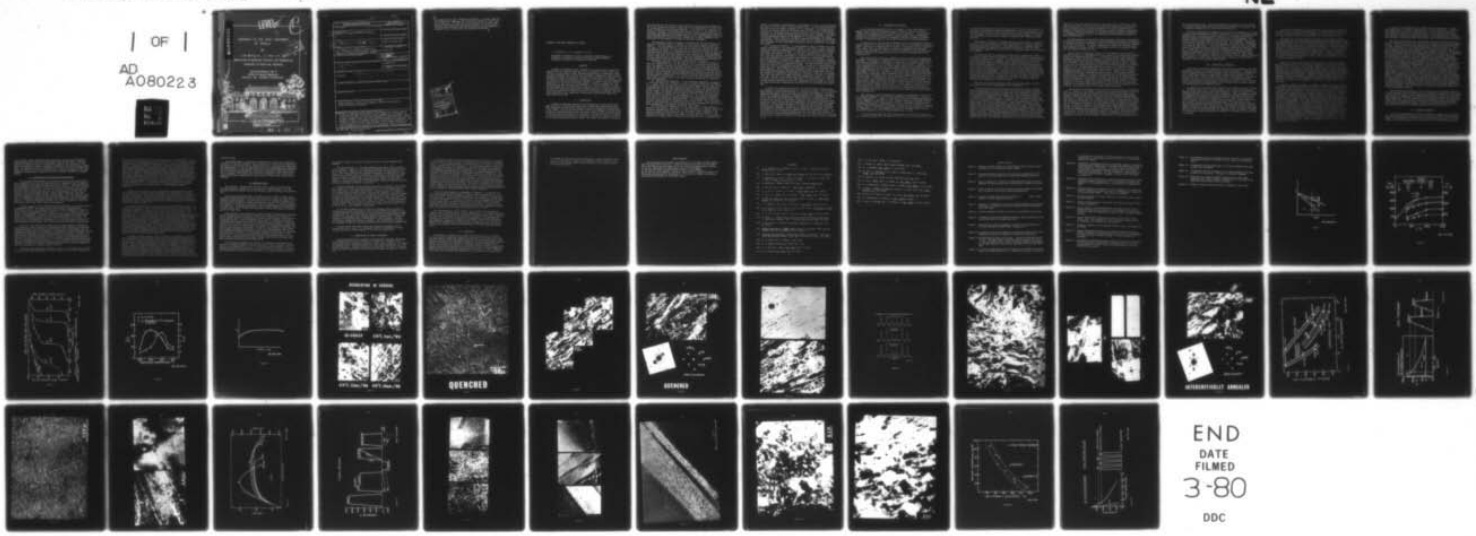

END
DATE
FILMED
3-80
DDC

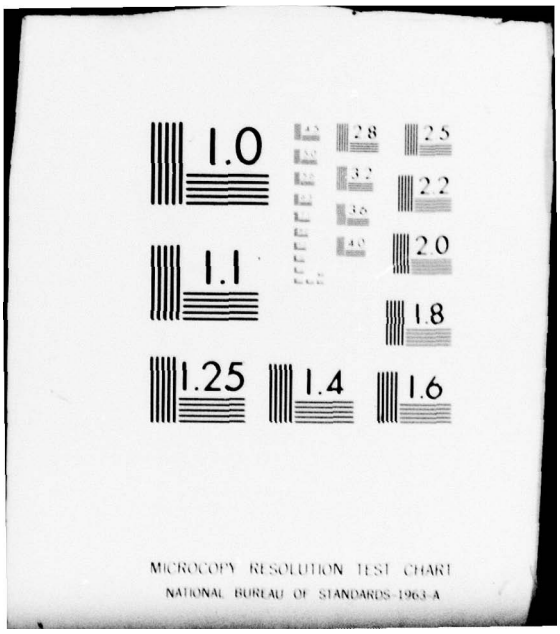
1.0
1.1
1.25
1.4
1.6
2.8
3.2
3.6
4.0
2.5
2.2
2.0
1.8
MICROCOPY RESOLUTION TEST CHART
NATIONAL BUREAU OF STANDARDS-1963-A

LEVEL II

ADVANCES IN THE HEAT TREATMENT OF STEELS

By

J. W. Morris, Jr., J. I. Kim, C. K. Syn
Department of Materials Science and Engineering
University of California, Berkeley

Technical Report No. 9
Office of Naval Research
Contract No. N00014-75-C-0154

80 1 28 154

(9) Technical rept.

SECURITY CLASSIFICATION OF THIS PAGE (When Data Entered)

REPORT DOCUMENTATION PAGE

READ INSTRUCTIONS BEFORE COMPLETING FORM

1. REPORT NUMBER: 9
2. GOVT ACCESSION NO.
3. RECIPIENT'S CATALOG NUMBER

(6) 4. TITLE (and Subtitle): ADVANCES IN THE HEAT TREATMENT OF STEELS.

5. TYPE OF REPORT & PERIOD COVERED

6. PERFORMING ORG. REPORT NUMBER

(10) 7. AUTHOR(s): J. W. Morris, Jr., J. I. Kim and C. K. Syn

8. CONTRACT OR GRANT NUMBER(s): N00014-69-A-0200-1062

9. PERFORMING ORGANIZATION NAME AND ADDRESS
J. W. Morris, Jr., Professor of Metallurgy
Dept. of Materials Science & Mineral Engineering
University of California, Berkeley, CA 94720

10. PROGRAM ELEMENT, PROJECT, TASK AREA & WORK UNIT NUMBERS: NR 031-762

11. CONTROLLING OFFICE NAME AND ADDRESS

(11) 12. REPORT DATE: Jul[illegible]979

13. NUMBER OF PAGES: 48 (12) 51

14. MONITORING AGENCY NAME & ADDRESS (if different from Controlling Office): (14) TR-9

15. SECURITY CLASS. (of this report): Unclassified

15a. DECLASSIFICATION/DOWNGRADING SCHEDULE

16. DISTRIBUTION STATEMENT (of this Report)
Unlimited

(15) N0001 4-75-C-0154,
N0001 4-69-A-0200-1062

17. DISTRIBUTION STATEMENT (of the abstract entered in Block 20, if different from Report)

18. SUPPLEMENTARY NOTES

19. KEY WORDS (Continue on reverse side if necessary and identify by block number)
Normal tempering, intercritical tempering, intercritical annealing, austenite reversion, martensite

20. ABSTRACT (Continue on reverse side if necessary and identify by block number)
A number of important recent advances in the processing of steels have resulted from the sophisticated uses of heat treatment to tailor the microstructure of the steels so that desirable properties are established. These new heat treatments often involve the tempering or annealing of the steel to accomplish a partial or complete reversion from martensite to austenite. The influence of these reversion heat treatments on the product microstructure and its properties may be systematically discussed in terms of the heat treating temperature in relation to the phase diagram. From this perspective,

DD FORM 1 JAN 73 1473 EDITION OF 1 NOV 65 IS OBSOLETE
S/N 0102 LF 014 6601

SECURITY CLASSIFICATION OF THIS PAGE (When Data Entered)

406 134

JOB

four characteristic heat treatments are defined: (1) normal tempering, (2) intercritical tempering, (3) intercritical annealing, and (4) austenite reversion. The reactions occurring during each of these treatments are described and the nature and properties of typical product microstructures discussed, with specific reference to new commercial or laboratory steels having useful and exceptional properties.

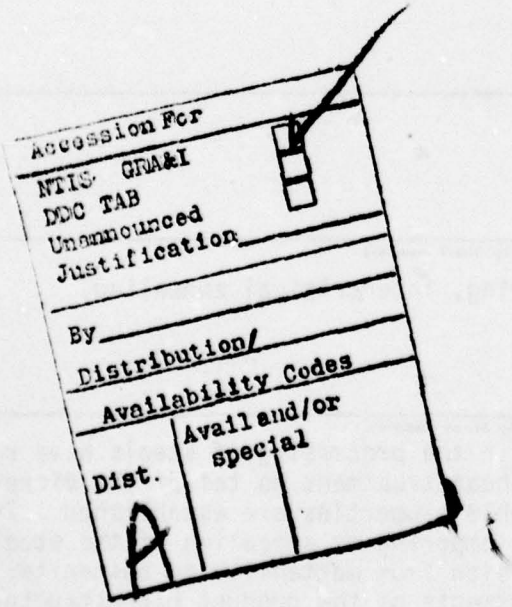

ADVANCES IN THE HEAT TREATMENT OF STEELS

J. W. Morris Jr., J. I. Kim and C. K. Syn

Department of Materials, Science and Mineral Engineering, and Materials and Molecular Research Division, Lawrence Berkeley Laboratory, University of California, Berkeley

ABSTRACT

A number of important recent advances in the processing of steels have resulted from the sophisticated uses of heat treatment to tailor the microstructure of the steels so that desirable properties are established. These new heat treatments often involve the tempering or annealing of the steel to accomplish a partial or complete reversion from martensite to austenite. The influence of these reversion heat treatments on the product microstructure and its properties may be systematically discussed in terms of the heat treating temperature in relation to the phase diagram. From this perspective, four characteristic heat treatments are defined: (1) normal tempering, (2) intercritical tempering, (3) intercritical annealing, and (4) austenite reversion. The reactions occurring during each of these treatments are described and the nature and properties of typical product microstructures discussed, with specific reference to new commercial or laboratory steels having useful and exceptional properties.

I. INTRODUCTION

A number of important advances in the processing of steels which have been made over the past twenty years have involved the sophisticated use of heat treatment to control the microstructure and consequently the properties of the steel. Some of the most useful of these new treatments involve variations on a simple elementary step: the alloy, which has been initially cooled or quenched to form a ferritic or martensitic starting structure, is reheated to an intermediate temperature to accomplish a partial or complete reversion to the high temperature austenite phase. The nature and extent of the rever-

sion reaction and the details of the associated microstructural changes may, of course, depend in a rather complex way on the composition of the alloy and on the heating and cooling rates employed. If we restrict our attention to alloys of relatively low interstitial content, however, it is possible to distinguish a sequence of characteristic microstructural changes which occur as the reheating temperature is raised relative to the phase diagram of the steel. These characteristic microstructural changes form a useful framework for a discussion of the response of steels to reheating treatments.

The elementary types of response to reheating may be classified by considering a prototypic alloy, a portion of whose phase diagram is shown as Figure 1. Let the composition of the alloy be given by the vertical line in the figure, and assume that the alloy has initially been quenched to form a martensite structure. Let the alloy now be reheated to one of the four temperatures noted along the isocomposition line, held at the selected temperature for some time, and then recooled to room temperature, using heating and cooling rates which are sufficiently rapid that decomposition during the heating and cooling steps can be ignored. The four temperatures noted along the isocomposition line then define four characteristic reactions:

(1) Normal Tempering. If the steel is held at a temperature which is below the temperature at which the formation of the austenite phase begins then the expected reactions are those associated with normal tempering, and which are familiar from the technology of plain carbon and maraging steels. The steel may harden through the formation or reconfiguration of small precipitates, such as carbides, and may simultaneously recover through the equilibration of point defects and the relaxation of dislocations introduced during the martensite transformation. It is well known that the properties of such steels may be adjusted over a very wide range by controlling the tempering time and temperature.

(2) Intercritical Tempering. If the reheating temperature is adjusted to the point marked (2) in Figure 1, which is slightly within the two phase $\alpha + \gamma$ region, then the reactions occurring during tempering will also involve a precipitation of the high temperature austenite phase. If the tempering conditions are such that the austenite phase can equilibrate insofar as its solute content is concerned then the precipitated austenite will be rich in solute, relatively stable, and may hence be retained in the microstructure after the alloy is returned to room temperature. The final microstructure will then be a mixture of tempered martensite and precipitated austenite retained in the metastable austenite phase. The consequences of this intercritical tempering will be discussed in more detail below. This treatment is basic in the production of typical structural steels intended for use at cryogenic temperature, for example, commercial "9Ni" steel.

(3) Intercritical Annealing. If the reheating is to the temperature marked (3) in Figure 1, near the top of the two phase $\alpha + \gamma$ region, then a more extensive decomposition will occur. A much higher volume fraction of the austenite phase is anticipated and this austenite phase, according to the equilibrium diagram, will be much leaner in solute species. If the reheating temperature is high enough the precipitated austenite will be unstable with

respect to martensite transformation on subsequent cooling to room temperature, and most of it will revert to the martensite phase. In this case the product microstructure will consist primarily of two components: a well-tempered martensite, or ferrite, which is relatively lean in solute, and a fresh martensite which is relatively high in solute and which is produced by the retransformation of the austenite precipitated during the heat treatment. The intercritical annealing reaction is fundamental to the processing of so-called "dual phase" steels, which are now under extensive development for automotive applications. Intercritical annealing is also used in combination with other heat treatments in the processing of specialty alloys intended for low temperature use.

(4) Austenite Reversion. If the martensitic steel is heated at a reasonably rapid rate to the temperature marked (4) in Figure 1, which lies well within the austenite stability field, then the alloy will undergo a complete reversion to the austenite phase. If the alloy is relatively rich in austenite stablizing solutes, so that the reversion temperature need not be too high, then the reverse transformation to austenite will occur predominantly by a shear mechanism which reverses the martensitic transformation. If the steel in question is a martensitic steel, that is if its martensite transformation temperatures lie above room temperature, then the austenite transformation will be reversed on subsequent cooling. The final microstructure of the steel will then be predominantly martensitic, but may have a finer effective grain size and a much higher dislocation density because of the double-shear transformation. If the steel is an austenitic steel, in the sense that its martensite transformation temperatures lie below room temperature, and if it was originally transformed to martensite by cooling to some very low temperature, then the steel will remain austenitic after being returned to room temperature. Because of the double shear transformation, however, the austenitic steel will now contain a very high density of internal defects. The reversion reaction may hence be used to "transformation strengthen" an austenitic steel which would otherwise be relatively soft in the as-quenched condition.

Of these four elementary reactions, the normal tempering reaction has been familiar to steel metallurgists for a great many years. While increasing metallurgical sophistication has led to continued improvements in the use of tempering treatments and in the resulting properties of tempered or maraged steel, the elementary features of normal tempering are reasonably well known. On the other hand treatments which involve the use of retransformation to austenite as a method of achieving a desirable final microstructure are more recent in origin, and are only now beginning to be understood and efficiently exploited. In the following sections we shall discuss the three prototypic types of such treatments: intercritical tempering, intercritical annealing, and austenitic reversion, in more detail using specific examples of their utilization in the processing of research alloys and commercial steels. The illustrations will be drawn primarily from our own recent work and that of others at the Lawrence Berkeley Laboratory, not with the implication that this is the only, or even the best work in the area, but rather it is most familiar to us.

II. INTERCRITICAL TEMPERING

If an initially martensitic alloy is reheated to the point marked (2) in Figure 1, just within the two-phase region, and held, then a solute-rich γ-phase will precipitate within the matrix of the initial α'. If the solute content of this precipitated austenite is sufficiently high a substantial fraction of it will be retained on subsequent cooling to create a two-phase mixture of tempered martensite and retained austenite at room temperature.

A typical use of intercritical tempering is in the processing of ferritic alloys intended for structural use at low temperature, including the established Fe-Ni[1-4] and recently developed Fe-Mn[5] grades. The simplest case is commercial "9Ni" steel, which is often used in a quench-and-tempered (QT) condition. Alloys which are leaner in nickel or which are intended for service under more extreme conditions are usually given a more elaborate treatment before the tempering step.

The intercritical tempering treatment is used to improve low-temperature toughness, principally by lowering the ductile-brittle transition temperature. The change in toughness on tempering is sensitive to the carbon content of the alloy and perhaps also to the content of other interstitials. Figure 2 contains superimposed plots of the Charpy impact energy (C_v) and plane-strain fracture toughness (K_{IC}) of 9Ni steel containing $\sim$0.06C in the quenched (Q) and quench-and-tempered (QT) conditions[6]. The intercritical temper accomplishes two changes in this case; it lowers the ductile-brittle transition temperature (DBTT) and it raises the "shelf" toughness of the alloy tested above the DBTT. Figure 3 shows a comparable plot for a research Fe-8Ni-2Mn-0.25Ti alloy[7] which was "gettered" of interstitials through the addition of titanium and given a cyclic initial heat treatment to refine its grain size before tempering. The intercritical temper also lowers the DBTT in this case, but does not sensibly affect the shelf toughness above the DBTT. These results are typical; a suitable intercritical temper always seems to have a beneficial effect on the ductile-to-brittle transition, but influences toughness above the DBTT (at a given strength level) only if the alloy contains a reasonable concentration of free interstitials.

The lowering of the ductile-brittle transition temperature on intercritical tempering depends on the time and temperature of tempering as well as on alloy composition[8,9]. Figure 4 illustrates the effect of tempering temperature on the toughness of 9Ni steel at 77°K. Optimum results are obtained when the tempering temperature is high enough to obtain a reasonable concentration of precipitated austenite, but low enough to insure that the austenite is rich in solute. Figure 5 illustrates the effect of tempering time at given temperature on toughness at 77°K. The toughness increases to a maximum value, but may eventually decrease if a very long tempering time is used.

In interpreting these and other consequences of intercritical tempering it is usually assumed that the dominant effects are due to the retention of the

austenite precipitated during the tempering step, though it should be kept in mind that the simultaneous tempering of martensite may also be important. The influence of retained austenite on toughness is a subject which has not been fully resolved. At the risk of some over-simplification, however, the results of recent research may be used to phrase a reasonably self-consistent interpretation.

The dominant influence of retained austenite appears to have two sources: it serves to getter deleterious interstitial species and it acts to refine the effective grain size of the alloy. The former effect is a dominant cause of the increased shelf toughness of carbon-containing alloys which have been intercritically tempered; the latter effect is a dominant cause of the decrease in the DBTT.

The carbon present in a martensitic steel may be contained as a supersaturation of free carbon in the matrix, if the steel has been rapidly quenched, or it may be gathered into clusters or carbide precipitates, if the steel has been more slowly cooled or tempered. In the former case the carbon is expected to form atmospheres along dislocations, inhibiting their mobility and hence decreasing toughness. In the latter case the carbides are preferential sites for void nucleation, with the result that ductile crack propagation is easier than it would otherwise be. Carbon is an austenite-stabilizing element, and is expected to aggregated in solution in the austenite during its precipitation, hence making the matrix relatively lean in carbon and relatively tough. The process can be observed directly when the steel contains a distribution of carbide precipitates prior to tempering. The composite Figure 6 shows the progressive dissolution of carbides as austenite is introduced during the intercritical tempering of a 6Ni-0.06C alloy.

The role of retained austenite in grain-refining martensitic alloys is more subtle, and is only now beginning to be understood[10].

The steels which are normally given an intercritical temper to improve their low temperature properties are Fe-Ni and Fe-Mn alloys which typically form a lath-martensite structure on quenching. This structure is illustrated by the optical micrograph shown in Figure 7 and the transmission electron micrograph shown in Figure 8. The fundamental element of the microstructure is a lath of dislocated martensite. As shown in the micrographs, these laths tend to be organized into packets of parallel laths; each prior austenite grain gives rise to one or a few such packets. Crystallographic analysis of the packet shows that, while packets are not always perfect, the laths within a packet tend to have only a slight misorientation with respect to one another. Laths in a packet hence tend to share common crystallographic planes, in particular, as illustrated in Figure 9, the (100) plane which is a common cleavage plane in bcc iron. Scanning fractographic analysis of Fe-Ni steels which have failed by cleavage below the DBTT indicates that local fracture often occurs through the cooperative cleavage of the aligned laths within a packet along a common (100) plane. The effective grain size of the alloy, insofar as cleavage

fracture is concerned, hence tends to be the packet size of the alloy rather than the lath size. Since the ductile-to-brittle transition in martensititic Fe-Ni and Fe-Mn alloys is usually associated with (and attributable to) a change in fracture mode from ductile rupture to quasi-cleavage, a significant decrease in the DBTT is expected if cleavage fracture is made more difficult by decreasing the packet size or by destroying the preferential alignment of laths within packets.

The decomposition of martensite packets through intercritical tempering is illustrated in Figure 10, which shows the preferential nucleation and retention of austenite along lath boundaries. Hence the martensite packets are decomposed in the as-cooled state. To insure resistance to cooperative cleavage during low-temperature testing, however, the decomposition of the martensite packet must be preserved during the test.

One of the more surprising results of recent research on the effect of retained austenite on toughness is that the austenite is almost never preserved during low temperature testing[11,12]. A virtually complete transformation of austenite is found during low temperature fracture of all steels studied to date (particularly 6Ni and 9Ni cryogenic steels) even when these are tested above the DBTT. This conclusion is documented in Figures 11 and 12. Figure 11 is a set of Mössbauer spectroscopy data taken from a specimen of 9Ni steel broken at 77°K. No measurable austenite is found in the fracture surface (upper curve) although a significant concentration of austenite is present in undeformed protions of the specimen (lower curve). Figure 12 is a profile transmission electron micrograph showing a section of the ductile fracture surface of this sample. No austenite is detected in the diffraction pattern, though regions resembling retained austenite are seen in the substructure. These have apparently transformed to a highly dislocated, ductile martensite. Associated studies[10] using tensile tests suggest that the austenite is transformed at a very early stage of deformation. The influence of precipitated austenite on toughness hence involves the properties of the austenite only indirectly, through the nature of its transformation products.

The austenite precipitation during intercritical tempering is transformed prior to fracture in two stages: a portion of the austenite reverts to martensite during cooling, and the remainder is mechanically transformed during testing. Recent research has shown that these two different transformation paths have decidedly different consequences, which are illustrated in Figures 13a and 13b. Figure 13a shows a sample of 6Ni steel in which austenite nucleated along lath boundaries, as in the 9Ni sample shown in Figure 10, but reverted to martensite on cooling. The transformation has an apparently pervasive memory, so that the thermally-reverted austenite regenerates the martensite variant which gave it birth. Lath alignment within the packet is re-established, and no effective grain refinement is achieved. Figure 13b shows a sample of 6Ni steel in which the austenite reverted to martensite during mechanical deformation. In this case the memory effect is apparently over-ridden by mechanical factors, and the austenite transforms to a variant compatible with

the local mechanical load. The crystallographic decomposition of the martensite packet is hence preserved after the re-transformation of austenite, with a consequent lowering of the ductile-brittle transition.

The above considerations suggest that intercritical tempering will be most beneficial when the austenite is finely distributed, so as to cause the maximum decomposition of the prior structure, and when it is stable with respect to thermally-induced transformation on cooling to the test temperature. The thermal stability of the austenite will be improved if the austenite is rich in solute and relatively small in particle size. The tempering temperature should thus be relatively low and the tempering time not too long, in keeping with practical experience. A fine distribution of austenite and a reasonable kinetics of austenite precipitation is promoted by high solute content (Ni or Mn). In 9Ni steel, the solute content is sufficiently high that a useful austenite distribution can be obtained by tempering the as-quenched alloy. Commercial 9Ni steel is hence often used in the QT condition. Less highly alloyed steels, for example, commercial 5-6Ni steels and the recently developed 5Mn composition, require prior heat treatment to achieve a suitable final structure, as will be discussed further below.

III. INTERCRITICAL ANNEALING

If a steel is initially quenched to form dislocated martensite, and then re-heated to a point in the upper portion of the two-phase $\alpha + \gamma$ region an extensive decomposition will occur forming a high volume fraction of austenite. At the same time the residual martensite is extensively tempered, and, at least in the case of Fe-Ni steels, takes on what is essentially a polygonized ferrite structure. When the alloy is returned to room temperature most (though not necessarily all) of the precipitated austenite reverts to martensite, creating what is predominantly a two-component microstructural mixture of fresh martensite and tempered ferrite.

An example of an intercritical annealed microstructure is shown in Figure 14. The alloy shown here is a 6Ni cryogenic steel. The highly dislocated regions within the structure are fresh martensite, formed by reversion of precipitated austenite on cooling to room temperature. The intermediate regions of relatively low dislocation content are tempered martensite, which may be reasonably well described as polygonized ferrite. Some retained austenite is also present, but is not included in the micrograph. As mentioned in the previous section, there is a pronounced memory to the martensite reversion reaction, andthe martensite particles tend to be very close in crystallographic orientation to the ferrite matrix. The martensite-ferrite interface appears coherent and clean, though the boundary between the highly dislocated martensite and the surrounding ferrite sometimes showns an apparent "leakage" of dislocations from the martensite, presumably to accomodate the transformation strain.

Intercritical annealing is used as one step in the thermal processing of cryogenic steels, as will be discussed below. Its principal application, however, is in the processing of the so-called "dual phase" steels[13] which are now under extensive, world-wide development for automotive applications.

The impetus for the development of dual-phase steels has its source in the increasing need for structural materials which permit weight reduction in automobiles without materially sacrificing performance or dramatically increasing manufacturing costs. The principal requirements for such an alloy call for high total tensile elongation, as a measure of formability, and high tensile strength, as a measure of fatigue and crush resistance[16]. It has become common to combine these criteria into a single figure of merit: the product of ultimate tensile strength and the total elongation. The steels which have the highest values of this "figure of merit" are the "dual phase" steels, which, as illustrated in Figure 15, offer a substantial advantage with respect to earlier automotive steels.

Despite the recent introduction of these new steels, whose publication history begins from the work of Hayami and Furukawa[13] in 1975 and of Rashid[17], published in the next year, their evident commercial potential has led to an extensive body of research in a great many laboratories, with the consequence that varieties of dual-phase steels having a wide range of compositions and heat treatments have been introduced, and the metallurgy of the alloys has rapidly become complex and sophisticated. Nonetheless the fundamental step in the heat treatment of the most common alloy remains a straightforward intercritical annealing, and many of the most important properties of these alloys can be discussed in terms of the consequences of intercritical annealing for microstructure.

Figure 16 contains a schematic of the heat treatment of an Fe-Si-C dual-phase steel taken from work by Koo and Thomas[18]. The heat treatment involves a quenching step followed by an intercritical annealing. The product microstructure is shown in Figure 17. It will be seen to resemble that obtained in intercritically annealed Fe-6Ni steel and presented in Figure 14. During the intercritical annealing step long islands of austenite form along the lath boundaries of the prior martensite. During subsequent cooling these revert into martensite, giving rise to the elongated regions of dislocated phase apparent in the micrograph. The highly dislocated regions are surrounded by a matrix of tempered ferrite. The interface between the ferrite and martensite is clean and coherent as illustrated by the lattice image of the interface[18] presented in Figure 18. As indicated in the figure, direct measurement of the local lattice parameter of the martensite phase shows a slight lattice expansion, which constitutes evidence for the expected accumulation of carbon in the martensite, a result of segregation of carbon to austenite during annealing. The transformation of precipitated austenite to martensite during cooling is not entirely complete; a small fraction of austenite is retained within the martensite phase. However, the available evidence suggests that this retained austenite has, at best, a secondary influence on the resulting properties of the steel.

As Davies[19] has emphasized, the ultimate tensile strength of a typical dual-phase steel is a nearly linear function of the volume fraction of martensite present and can be well estimated from a law of mixtures calculation. The exceptional ductility of dual-phase steels is more subtle in its origin and remains the subject of intensive research. The interpretation of ductility which appears to be emerging from this research may be briefly stated as follows.

The stress-strain curve of a typical dual-phase steel is shown in Figure 19, and illustrates that the bulk of the total elongation occurs prior to sample necking. The point at which the sample necks in tension can be predicted from its work hardening rate ($d\sigma/d\varepsilon$) from the Considere criterion $d\sigma/d\varepsilon = \sigma$. Hence the elongation prior to plastic instability is equal to that which occurs before the work hardening rate falls to equal the applied stress. The sustained high work hardening rate of dual-phase alloys appears to arise from two factors: the microstructure consists of an intimate mixture of relatively soft and relatively hard components, and both components are plastically deformable. As the dual-phase steel is loaded the initial deformation is largely confined to the ferrite phase, which is relatively soft and ductile due both to its relatively low average dislocation density and to a relatively low interstitial content as a consequence of segregation of interstitials to the precipitated austenite during annealing. Since the deformation of this soft ferrite is constrained by adjacent regions of hard phase the rate of dislocation multiplication within it, and hence its work hardening rate, will be rather high. The consequence is that one achieves a significant amount of plastic elongation before the deformation of the martensite has begun to occur to any significant degree. Continued work hardening of the ferrite eventually causes its strength to exceed the yield strength of the neighboring martensite, at which point the martensite begins to undergo significant plastic deformation with accompanying work-hardening, and one achieves a second increment to the tensile elongation in which the sample is deforming more or less as would a uniform phase of high dislocation density. The sum of these two regimes of plastic flow results in a high prenecking elongation.

The post-necking elongation is also promoted by the dual-phase structure. If the hard phase within the steel were an incompatible constituent, for example a large carbide, then one would expect tensile failure to occur at a relatively early stage in deformation due to decohesion between the ferrite matrix and the hard constituent, or due to cracking of the constituent itself. In dual phase steels which have been treated to achieve good interfacial cohesion between the ferrite and martensite element, however, no such decohesion is observed and the alloy exhibits a reasonable post-necking ductility as well.

IV. AUSTENITE REVERSION

If an initially martensitic alloy is heated to a temperature well within the austenite stability field then the structure will revert to the austenite phase. If the heating is carried out at a sufficiently rapid rate, or if the austenite reversion temperature is sufficiently low, then the reversion will

occur through a shear mechanism which essentially reverses the martensitic transformation which created the martensite structure initially. Austenite reversion treatments have been traditionally used for many purposes in the thermal processing of steels, including normalization and initial grain refinement. The present review will emphasize two recent, and rather different applications which lead to alloys having unique or unusual properties: the transformation strengthening of austenite and the reversion treatment of maraging steels.

A. Transformation Strengthening of Austenite.

To transformation-strengthen an austenitic alloy one must begin with an alloy composition such that the martensite start temperature (M_s) is between room temperature and liquid nitrogen temperature (-196°C). The alloy may then be transformed to martensite (at least in part) by cooling in liquid nitrogen. The martensitic alloy is then reverted to austenite by heating to above the austenite finish temperature (A_f) at a rate rapid enough to insure that the reversion reaction proceeds through a reverse shear mechanism rather than through a diffusional nucleation and growth process. When the reversion reaction is complete the alloy is cooled to room temperature. The reverted austenite is, in general, appreciably stronger than annealed austenite due principally to an increased dislocation density and to the formation of a fine substructure[21] due to the reverse shear transformation.

Initial research on the transformation strengthening of austenite was done by Krauss and Cohen[21] who demonstrated transformation strengthening in Fe-(30-34)Ni alloys, and obtained an increase in yield strength from approximately 30 ksi to approximately 60 ksi after a $\gamma \rightarrow \alpha' \rightarrow \gamma$ reversion cycle. In further work Koppenaal[22] obtained a yield strength increase from approximately 40 ksi to approximately 105 ksi by reverting an Fe-24Ni-4Mo-0.3C alloy, and showed that the yield strength could be further increased, to ~160 ksi. In this case the strengthening is presumably due to the simultaneous influence of transformation induced defects and carbide precipitates formed during heating.

While the work cited above suggested that transformation strengthening could provide a useful alternative to thermomechanical treatment in processing austenitic steels, the approach suffered from the dual disadvantages that the strengths obtained were not exceptional in comparison to those obtainable through deformation processing or precipitation hardening from austenitic steels, and that the heat treatment employed required a very rapid heating, impractical in alloys to be used in other than very thin sections. These drawbacks appear to have been overcome in work by Jin et. al.[23] which combined precipitation hardening with transformation strengthening to achieve austenitic alloys having yield strengths in excess of 180 ksi, using heating rates which should be compatible with the processing of relatively thick sections.

The alloy most extensively studied by Jin et. al. had composition Fe-33Ni-3Ti and was processed according to the heat treatment cycle shown in Figure 20.

The evolution of microstructure during heat treatment is illustrated by the sequences of optical micrographs shown in Figure 21. In the annealed condition the alloy has a large grain size and contains a low density of internal dislocations. Ausaging at 720°C for four hours introduces a uniform dispersion of fine, spherical $\gamma(Ni_3Ti)$ precipitates, which are coherent with the matrix and contribute a substantial precipitation hardening. The yield strength of the alloy in the annealed condition is 50 ksi; after ausaging the yield strength increases to 144 ksi. The ausaging has the second consequence that the martensite start temperature of the alloy increases monotonically during aging due to depletion of nickel from the matrix. The M_s temperature, which is initially below liquid nitrogen temperature, increases to approximately -70°C at the end of the ausaging treatment. An optical micrograph of the ausaged structure is shown in Figure 21a. A transmission electron micrograph of the ausaged structure showing the distribution of the γ' precipitates is given in Figure 22a.

Because of the increase in the M_s temperature during ausaging the alloy could subsequently be transformed to martensite by refrigeration in liquid nitrogen. Cooling in liquid nitrogen produces a microstructure which contains ∿60% martensite phase. An optical micrograph showing the resulting dense distribution of martensite plates is presented in Figure 21b. A corresponding transmission electron micrograph, which reveals that the martensite is internally twinned, is shown in Figure 22b.

Following refrigeration in liquid nitrogen the alloy could be reverted to austenite by heating to 720°C at a controlled heating rate of ∿8°C/minute. The reheating accomplishes a complete reversion of the martensite phase. After subsequent cooling to room temperature the reverted austenite has a yield strength of 173 ksi, indicating a significant increment in strength due to the transformation. An optical micrograph of the reverted alloy is shown in Figure 21C. While this alloy is entirely austenitic there remain martensite-like features within the microstructure, which are ghosts of the martensite formed on refrigeration in liquid nitrogen. Transmission electron microscopic studies, as illustrated in Figure 22C, show that these martensite-like features are regions of very high dislocation density, presumably created by the reverse shear transformation of the martensite particles. The structure of the alloy hence consists of a mixture of highly dislocated austenite which arose from the retransformation of the martensite phase and very soft dislocation-free austenite which corresponds to the untransformed matrix.

Very high strength austenitic alloys can hence be obtained by transformation strengthening a matrix which has previously been precipitation hardened. The use of a precipitation-hardened alloy has the additional advantage that the transformation-induced defects are very stable to annealing at elevated temperature. Figure 23 shows a transmission electron micrograph of a region of the austenite which was reverted and held at 720°C for 7 hours. There is only a very slight deterioration in yield strength after this extended holding. Transmission electron micrographic studies show that the highly dislocated region remained intact and stable during annealing. There is, however, some evident fuzziness in the periphery of these regions after 7 hours of annealing, indicating a gradual leakage of transformation-induced dislocations into the surrounding

austenite phase.

The disadvantage of transformation-hardening as a means of strengthening austenite is that the treatment is only applicable to alloys whose compositions had been so adjusted that the M_s temperatures lie in an appropriate range below room temperature. It is also important that after transformation strengthening has been carried out the product austenite has sufficient mechanical stability that it does not catastrophically transform to martensite under elastic load, or the strength of the alloy will be low and determined by the stress which induces martensite transformation rather than the stress which causes plastic yielding.

B. Maraging Steels

The reversion treatment has also been used to achieve unusually high strength-toughness combinations in conventional maraging steels. The work described here was carried out by Jin and Morris, and is described in reference (24).

The so-called maraging steels are alloys of iron, nickel, cobalt, molybdenum and titanium which are low in carbon and known to have very good strength-toughness characteristics. The alloys are usually processed by quenching to form martensite followed by normal tempering to bring out precipitation hardening species, which may be Mo clusters, Ni-Mo precipitates, or other intermetallic compounds. A further improvement in the strength-toughness charactersitics of these alloys would, however, be desireable, and has been sought by investigators for some time.

Early research toward improved strength-toughness combinations in maraging steels concentrated on attempts to improve the toughness of the steels at a given strength level by introducing an austenite phase through an intercritical tempering treatment. While researchers have reported toughness improvements in maraging steels associated with the introduction of austenite a closer examination of this data[25] reveals that either the apparent toughness improvement results from a loss of alloy strength or depends on toughening mechanisms other than the introduction of austenite. A specific investigation of the change in the strength-toughness characteristic of the 250 grade maraging steel on the introduction of austenite by intercritical tempering[25] shows that the austenite has essentially no effect on the strength-toughness characteristic. This result is, of course, consistent with results obtained from research on cryogenic steels, and reported in section II, when these steels are tested above their ductile-brittle transition temperatures.

A more successful approach to improve the toughness of maraging steels employs a reversion treatment, and has been used by Jin and Morris[24] and also, implicitly, by Antolovich et. al.[26]. In this approach the steels are first maraged to establish a precipitate distribution, rapidly reverted to austenite and retransformed to martensite to establish a very high dislocation density,

and finally re-aged to stabilize the high dislocation density against early yielding.

The microstructure of a 250 grade margaing steel aged at 550°C for five hours is shown in Figure 24. The maraged precipitates in the martensite matrix are clearly seen. These proved to be primarily Ni_3Mo with some admixture of Ni_3Ti. When the martensite with embedded precipitates is subjected to a rapid reversion to austenite and retransformed to martensite an extremely high dislocation density is established. This dislocation density is illustrated in Figure 25. Also present in the microstructure are discrete islands which appear as large white particles in the micrograph. These are retained austenite particles, and make up ∿10-15% of the alloy.

From the appearance of the microstructure shown in Figure 25, particularly with respect to its very high dislocation density, one would expect that the alloy would have a very high yield strength. In fact, the yield strength of the maraging steel decreases slightly on reversion treatment. An analysis of the stress-strain curve for the alloy suggests that the decreased yield strength is due to an incipient yielding at a rather low stress level. This incipient yielding may be attributed to the very high density of fresh dislocations, some of which are apparently mobile under rather low stresses. To pin these dislocations and increase the strength the alloy was given a second low temperature aging at 380°C. This secondary low-temperature aging adds an increment of 30 to 50 ksi in the yield strength of the alloy.

The strength-toughness data for 250 grade maraging steels processed by maraging plus reverse transformation plus secondary aging are compared to the strength-toughness characteristics of alloys processed through normal maraging in Figure 26. As can be seen from the figure the reverse transformation does produce an improvement in the strength-toughness characteristic. A fracture toughness in the neighborhood of 160 ksi$\sqrt{in}$ at a yield strength of 200 ksi was achieved through the reversion treatment. This combination of strength and toughness exceeds any previously published for the 250 grade maraging steel.

It would appear from these results that reversion treatments can be successfully used to improve the strength-toughness characteristics of high strength structural steels intended for use near room temperature.

V. COMBINATIONS OF THERMAL TREATMENTS.

The characteristic heat treatments which have been discussed individually in preceding sections can also be used in combination to establish alloys having particularly desirable properties. Cyclic heat treatments, for example, are commonly used in the processing of specialty alloys intended for use under extreme conditions. Examples include the so-called QLT, 2B, and 2BT treatments which have been found useful in the processing of steels intended for cryogenic use.

Low nickel cryogenic steels, including both the 5Ni "Cryonic 5" produced by the Armco Steel Co., and the 5.5Ni cryogenic steel produced by the Nippon Steel Co., are processed through a treatment which, in the case of the Nippon alloy, is known as the QLT treatment.[27] The processing sequence consists of a quenching followed by an intercritical annealing followed by an intercritical tempering to introduce retained austenite. It is found that while the intercritical tempering does not itself improve cryogenic properties it substantially improves the cryogenic toughnesses which can be obtained by a subsequent intercritical tempering. The advantage introduced by the intermediate intercritical anneal is not yet fully understood. Our preliminary research indicates, however, that alloys which have been intercritically annealed will establish a much finer and more uniform distribution of precipitated austenite on subsequent intercritical tempering. The reason is believed to lie in the nickel segregation associated with the intercritical annealing step, which provides a density of sites relatively high in nickel content at which austenite can easily precipitate during subsequent intercritical tempering.

The 2B cycling treatment is diagrammed in Figure 27. It consists of a four step thermal cycling treatment in which austenite reversions are alternated with intercritical annealing treatments. Its purpose is to grain refine the alloy matrix, and it has been found successful in reducing the grain size of Fe-Ni[28] and Fe-Mn[29,5] steels to ~1 micron. The 2B treatment was initially used to grain-refine Fe-12Ni-0.25Ti alloys so that they would retain high toughness with good structural strength in liquid helium. It was found that 12Ni steel processed through the 2B treatment would retain toughnesses greater than 200 ksi $\sqrt{in}$ at yield strength near 200 ksi at 4.2 - 6°K.[30]

The 2B treatment by itself, however, has not been found sufficient to toughen alloys containing carbon for low temperature use. In carbon-containing alloys it is necessary to add an intercritical tempering after the 2B treatment has been used to establish a very fine grain structure. The resulting 2BT treatment was shown to be sufficient [6] to establish an excellent combination of strength and toughness in commercial 9Ni steel at 4-6°K. In very recent research this treatment has also been shown to establish a good combination of strength and toughness in Ni-free Fe-5Mn alloys [5] at liquid nitrogen temperature.

VI. CONCLUSION

The examples described in this paper were put forward for two reasons: To illustrate the significant advances in properties of steel which have been obtained recently through the sophisticated use of heat treatment and to simultaneously illustrate the fundamental simplicity of the heat treatments employed. Despite the simplicity of these heat treatments, and the emerging general picture of the associated changes in the microstructures of steels, it is nonetheless true that many features of the response of typical alloys through these characteristic heat treatments remain poorly understood. It may be expected that still futher advances and improvements in the properties of steels will

be obtained as continued research establishes a better fundamental undering of the response of steels to heat treatments which involve some reversion to the austenite phase, hence permitting a more precise control of the microstructures.

Acknowledgement

The preparation of this paper was supported by the Office of Naval Research under Contract N00014-75-C-0154. Research reported here draws on work supported by the Office of Naval Research, by the Division of Basic Energy Sciences of the U.S. Department of Energy under contract W-7405-Eng-48, by the Electric Power Research Institute under contract RP636-2, and by the Air Force Materials Laboratory under Contract F33615-73-C-5100. The The authors appreciated the assistance of J.Y.Koo and G. Thomas in providing illustrative micrographs of dual-phase steels.

REFERENCES

(1) C. W. Marshall, R. F. Heheman, and A. R. Troiano, Transactions Am. Soc. Metals, 55, 135 (1962)

(2) T. Ooka and K. Sugino, J. Japan Inst. Metals, 30, 435 (1977) (in Japanese).

(3) S. Nagashima, T. Ooka, S. Sakino, H. Mimura T. Fuzishima, S. Yano, and H. Sakurai, Trans. I.S.I.J., 11, 402 (1971).

(4) D. Sarno and J. Bruner, ARMCO Steel Corp., Private Communication.

(5) M. Niikura and J. W. Morris Jr., Met. Trans. (submitted).

(6) C. K. Syn, S. Jin and J. W. Morris Jr, Met. Trans., 7A, 1827 (1976).

(7) S. Jin, S. K. Hwang, and J. W. Morris Jr, Met. Trans., 6A, 1721 (1975).

(8) T. Ooka, H. Mimura, S. Yano, K. Sugino, and T. Toisumi, J. Japan Inst. Metals, 30, 442 (1966) (in Japanese).

(9) S. K. Hwang, S. Jin, and J. W. Morris Jr, Met.Trans., 6A, 2015 (1975).

(10) J. W. Morris Jr, C. K. Syn, J. I. Kim, and B. Fultz., Proceedings - ICOMAT -79, Cambridge, Mass., June, 1979.

(11) C. K. Syn, B. Fultz, and J. W. Morris, Jr, Met. Trans., 9A, 1635 (1978).

(12) B. Fultz, M.S. thesis, Dept. Materials Science and Mineral Engineering, U. California, Berkeley, 1978. (Lawrence Berkeley Lab, Rept. LBL-7671).

(13) S. Hayami and T. Furukawa, Proceedings, Microalloy-75, Washington, 1975, pp. 78-87.

(14) Modern Developments In HSLA Formable Steels (Proceedings: AIME Symposium Chicago, 1977) A.T. Davenport, Ed. (in press).

(15) Structure And Properties of Dual Phase Steels (Proceedings: AIME Symposium, New Orleans, 1979)R. C. Kot and J. W. Morris Jr, eds., (in press).

(16) R. G. Davies and C. L. Magee, in ref. (15).

(17) M. S. Rashid, SAE Preprint 760206, Feb. 1976.

(18) J. Y. Koo and G. Thomas, Met. Trans. 8A, 525 (1977).

(19) R. G. Davies, Met. Trans., 9A, 671 (1978).

(20) J. Y. Koo and G. Thomas, in reference 14.

(21) G. Krauss, Jr. and M. Cohen, Trans. TMS-AIME, 229, 1212 (1962).

(22) T. J. Koppenaal, Met. Trans., 2, 1549 (1972).

(23) S. Jin, J. W. Morris, Jr, Y.L. Chen, G. Thomas and R. I. Jaffe, Met. Trans., 9A, 1625 (1978).

(24) S. Jin and J. W. Morris, Jr, Rept. AFML-TR-75-119, May, 1975.

(25) S. Jin, D. Huang, and J. W. Morris, Jr, Met. Trans., 9A, 637 (1976).

(26) S. D. Antolovich, A. Saxena, and G. R. Chanini, Met. Trans., 5, 623 (1974).

(27) S. Yano, H. Sakurai, H. Mimura, N. Wakita, T. Ozawa, and K. Aoki, Trans. I.S.I.J., 13, J33, (1978).

(28) S. Jin, J. W. Morris, Jr, and V. F. Zackay, Met. Trans., 6A, 191 (1975).

(29) S. K. Hwang and J. W. Morris, Jr, Met. Trans.(in press).

(30) S. Jin, S. K. Hwang, and J. W. Morris, Jr., Met. Trans., 6A, 1569, (1975).

Figure Captions

Figure 1: Schematic drawing showing four characteristic heat treatment points in relation to the equilibrium phase diagram.

Figure 2: Fracture and impact toughness as a function of temperature for 9Ni steel in the as-quenched and intercritically-tempered conditions.

Figure 3: Impact toughness of a laboratory Fe-8Ni-2Mn-0.25Ti alloy is the as-quenched, and grain-refined plus intercritically tempered conditions.

Figure 4: Impact toughness at 77°K and retained austenite content in 9Ni steel as a function of intercritical tempering temperature.

Figure 5: Schematic drawing illustrating the change in impact toughness at 77°K with tempering at 550°C.

Figure 6: Sequence of transmission electron micrographs showing the progressive dissolution of carbides with austenite precipitation during tempering of 6Ni steel.

Figure 7: Optical micrograph drawing the structure of martensite in 6Ni steel.

Figure 8: Transmission electron micrograph showing the typical structure of dislocated martensite in quenched 9Ni steel.

Figure 9: Transmission electron micrograph of a packet of lath martensite in 6Ni steel showing the common (100) cleavage plane.

Figure 10: Transmission electron micrograph of a martensite packet in 9Ni steel showing the retention of austenite along the lath boundaries.

Figure 11: Mossbauer spectra taken from a Charpy specimen of 9Ni steel tested at 77°K. The upper curve is from the fracture surface; the second is from an etched surface. Neither shows the austenite peak present in the lower spectra, taken from an undeformed portion of the specimen.

Figure 12: A profile transmission electron micrograph of a ductile fracture surface in 9Ni steel broken at 77°K. The fracture surface is indicated.

No austenite is found near the fracture surface, though regions morphologically resembling retained austenite (e.g., the circled region) are common.

Figure 13: Comparative transmission electron micrographs showing the differing microstructural consequences of thermally and mechanically-transformed austenite in 6Ni steel. (a) After thermal transformation of austenite: the crystallographic alignment of laths within a packet is re-established. (b) After mechanical transformation at 77°K: the crystallographic alignment of laths within the packet is broken up.

Figure 14: Structure of 6Ni steel after intercritical annealing showing highly dislocated regions representive of re-transformed austenite and regions of low dislocation density representative of tempered ferrite.

Figure 15: Tensile strength as a function of total elongation for several commercially-available automotive steels, illustrating the superiority of the dual-phase grades. (After Davies and Magee[16]).

Figure 16: Schematic diagram of the heat treatment of dual phase steel (after Koo and Thomas[18]).

Figure 17: Optical microstructure of an Fe-Si-C dual phase steel after intercritical annealing.[18]

Figure 18: Lattice image of a ferrite-martensite interface in Fe-Si-C dual phase steel showing the coherence of the boundary and the lattice expansion within the martensite, presumably due to increased carbon content.

Figure 19: Typical engineering stress-strain curves of dual phase Fe-Si-C steels (4S1 - 4S3) compared to a 100% martensitic grade (4A) and to commercial Van 80 (after Koo and Thomas[20]).

Figure 20: Schematic diagram of the processing sequence used to strengthen Fe-Ni alloys.

Figure 21: Optical micrographs showing the evolution of the microstructure during transformation strengthening of Fe-33Ni-3Ti: (a) as-ausaged; (b) after cooling in liquid nitrogen; (c) after reversion to austenite.

Figure 22: Transmission electron micrographs showing the evolution of the microstructure during transformation strengthening of Fe-33Ni-3Ti (a) as-ausaged; (b) after cooling in liquid nitrogen; (c) after reversion to austenite.

Figure 23: Transmission electron micrograph showing retention of transformation-induced defects in Fe-33Ni-3Ti after seven hours holding at 720°C.

Figure 24: Transmission electron micrograph of 250 grade maraging steel aged at 550°C for five hours.

Figure 25: Transmission electron micrograph of 250 grade maraging steel aged at 550°C for five hours, then given a reversion treatment.

Figure 26: Comparison of strength-toughness characteristic of 250 grade maraging steels given reversion treatment (I,II) with that of the same steel after normal thermal treatments.

Figure 27: Thermal cycling procedure for grain refinement in 12Ni steel.

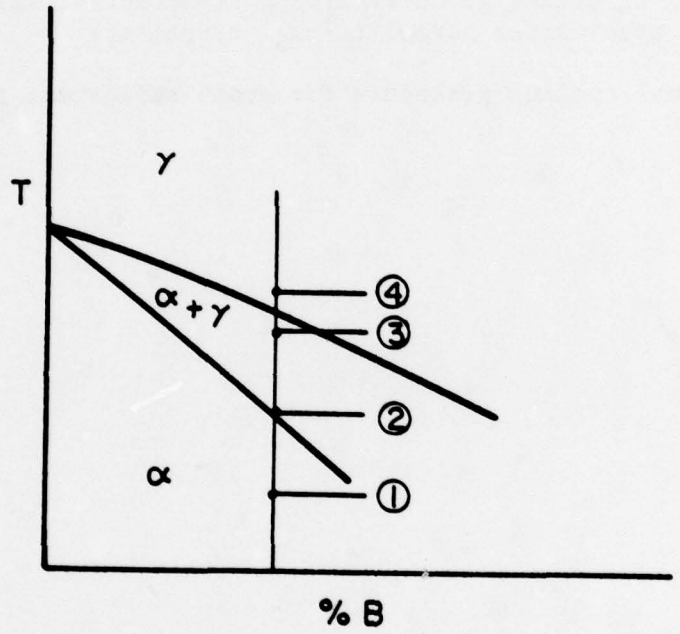

XBL796-6415

Figure 1

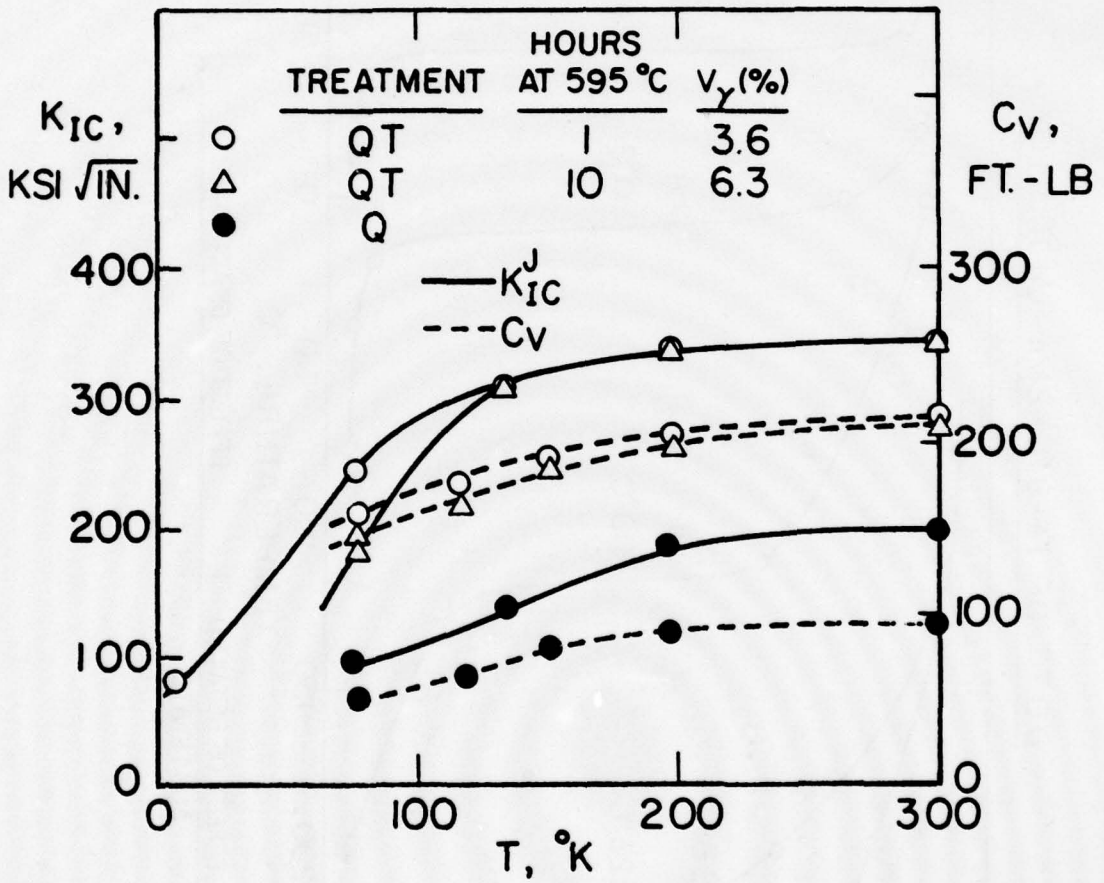

XBL 773-5138

Figure 2

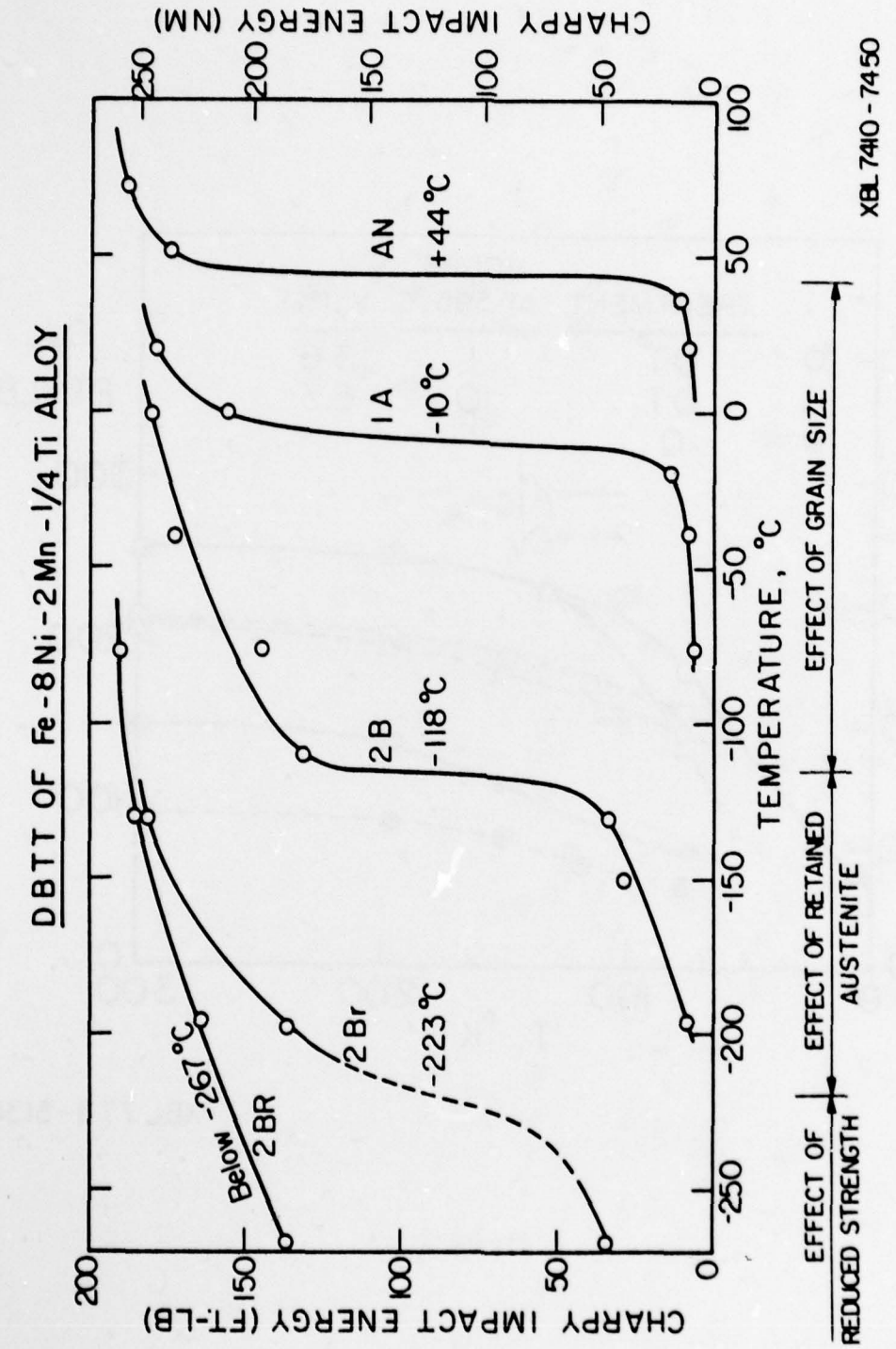
DBTT OF Fe-8Ni-2Mn-1/4 Ti ALLOY
CHARPY IMPACT ENERGY (FT-LB)
CHARPY IMPACT ENERGY (NM)
TEMPERATURE, °C
AN
+44°C
1A
-10°C
2B
-118°C
2Br
-223°C
2BR
Below -267°C
EFFECT OF REDUCED STRENGTH
EFFECT OF RETAINED AUSTENITE
EFFECT OF GRAIN SIZE
XBL 7410-7450

Figure 3

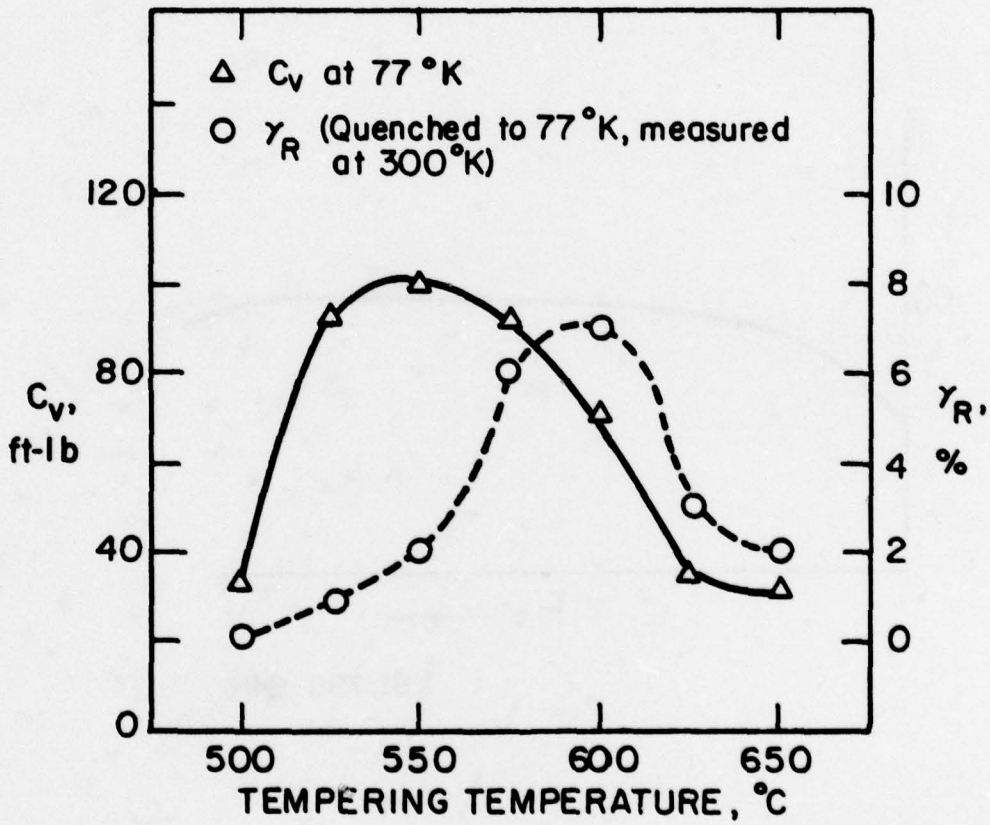
Δ C_v at 77 °K
O γ_R (Quenched to 77 °K, measured at 300°K)
120
80
40
0
C_v, ft-lb
10
8
6
4
2
0
γ_R, %
500
550
600
650
TEMPERING TEMPERATURE, °C
XBL796-6420

Figure 4

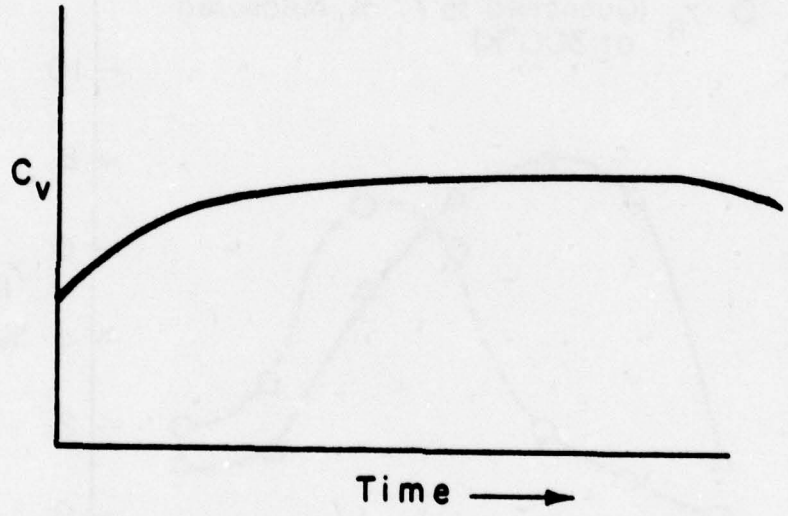

XBL 796-6416

Figure 5

DISSOLUTION OF CARBIDE

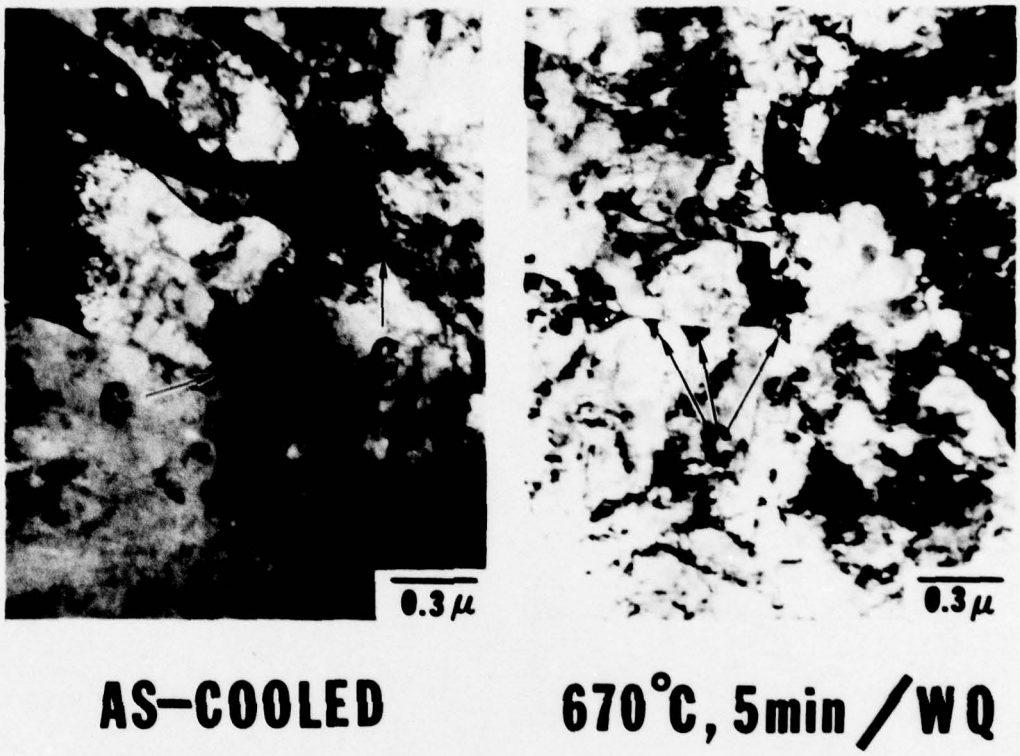

AS-COOLED

670°C, 5min / WQ

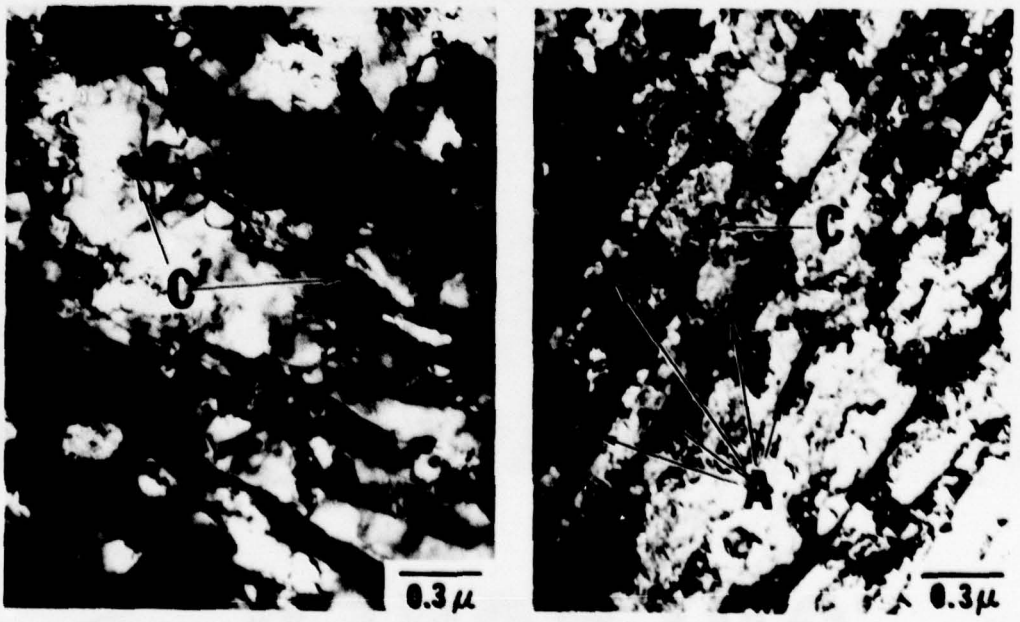

670°C, 15min / WQ

670°C, 30min / WQ

Figure 6

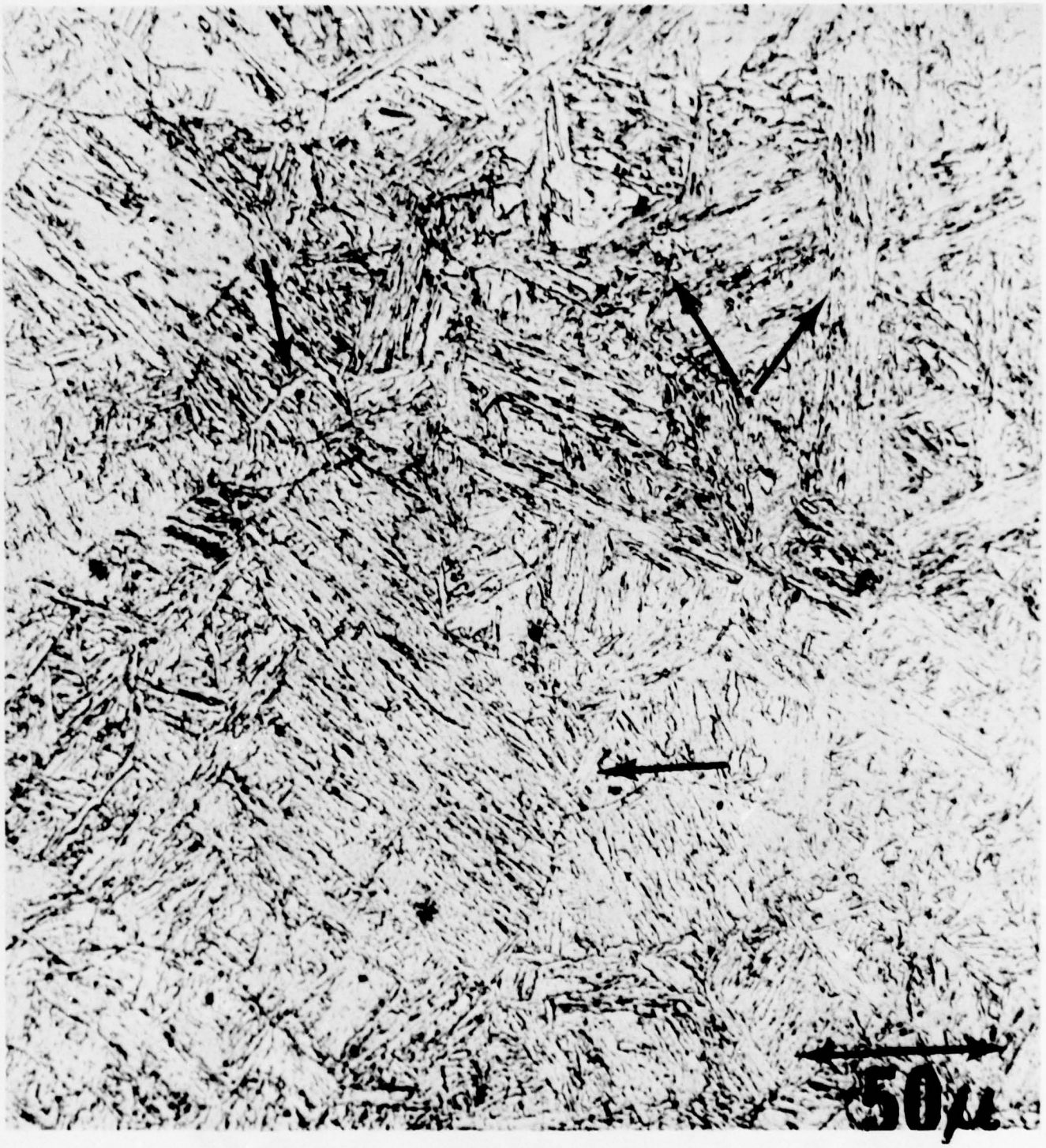

QUENCHED

Figure 7

Figure 8

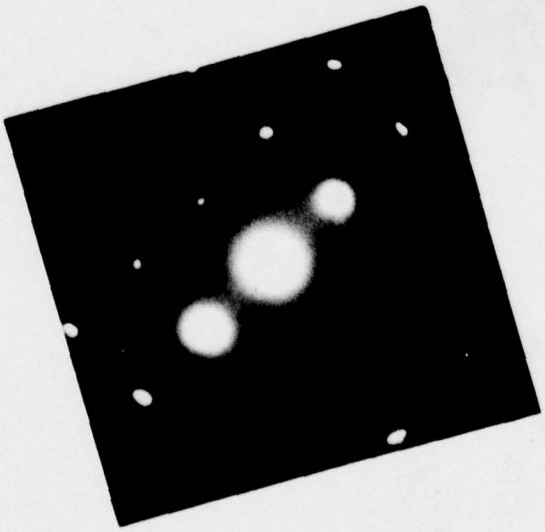

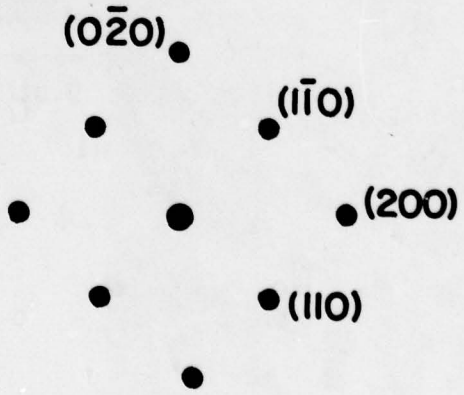

[001] martensite

QUENCHED

Figure 9

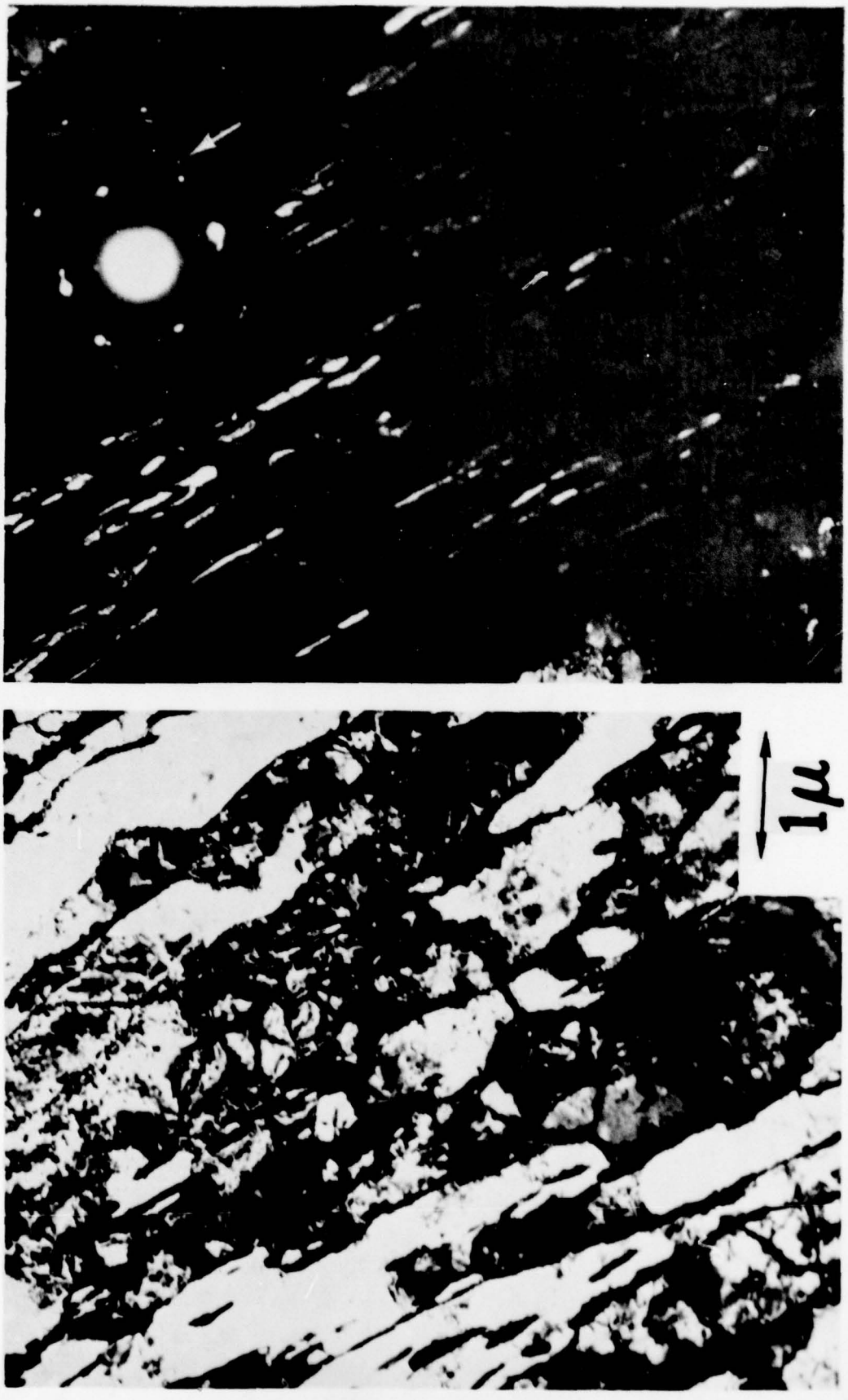

Figure 10

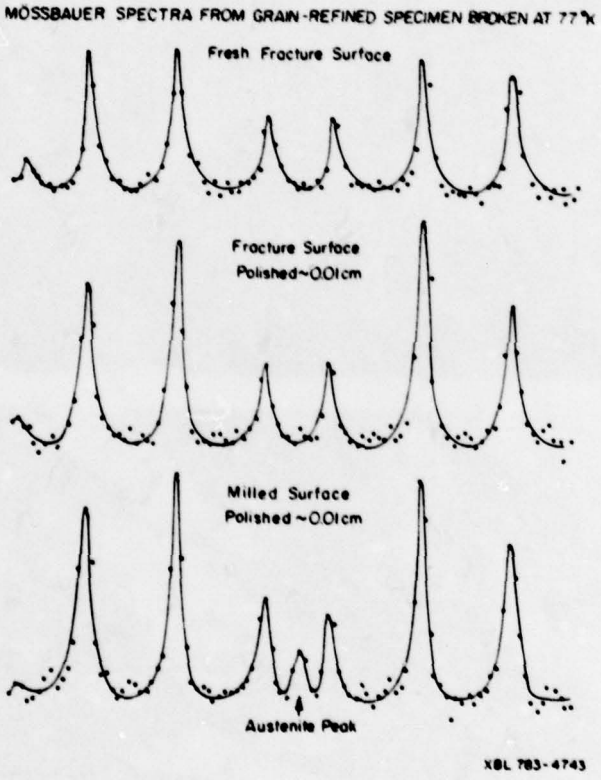
MÖSSBAUER SPECTRA FROM GRAIN-REFINED SPECIMEN BROKEN AT 77°K
Fresh Fracture Surface
Fracture Surface
Polished~0.01cm
Milled Surface
Polished~0.01cm
Austenite Peak
XBL 783-4743

Figure 11

Figure 12

(a)

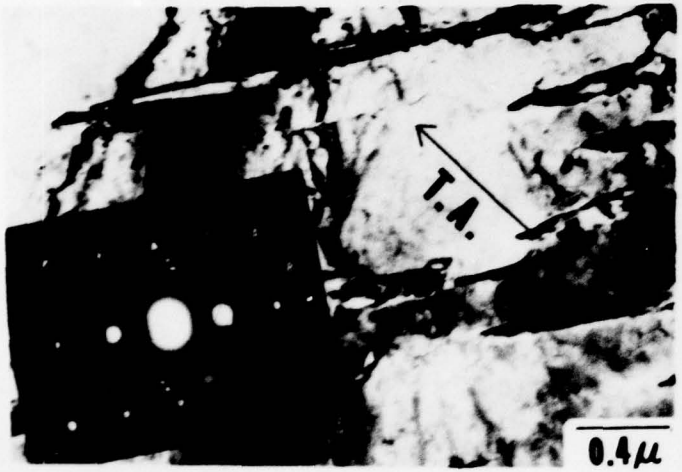

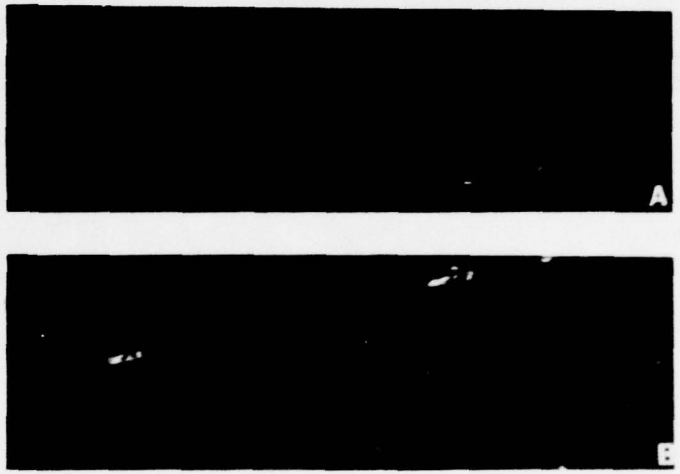

(b)

Figure 13

XBB794-5778

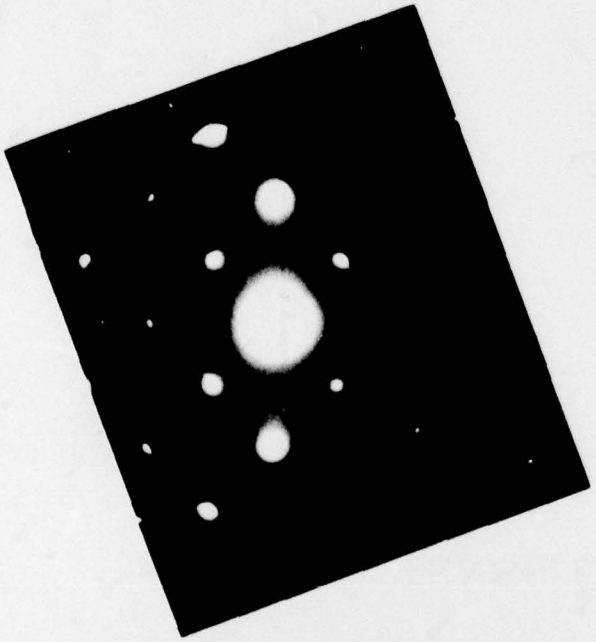

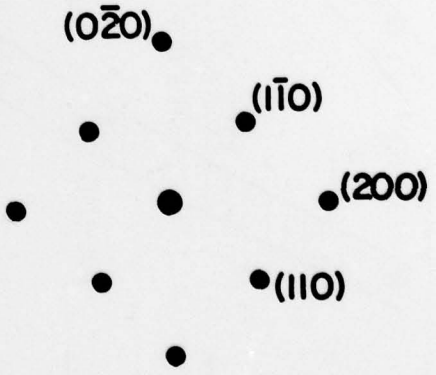

INTERCRITICALLY ANNEALED

Figure 14

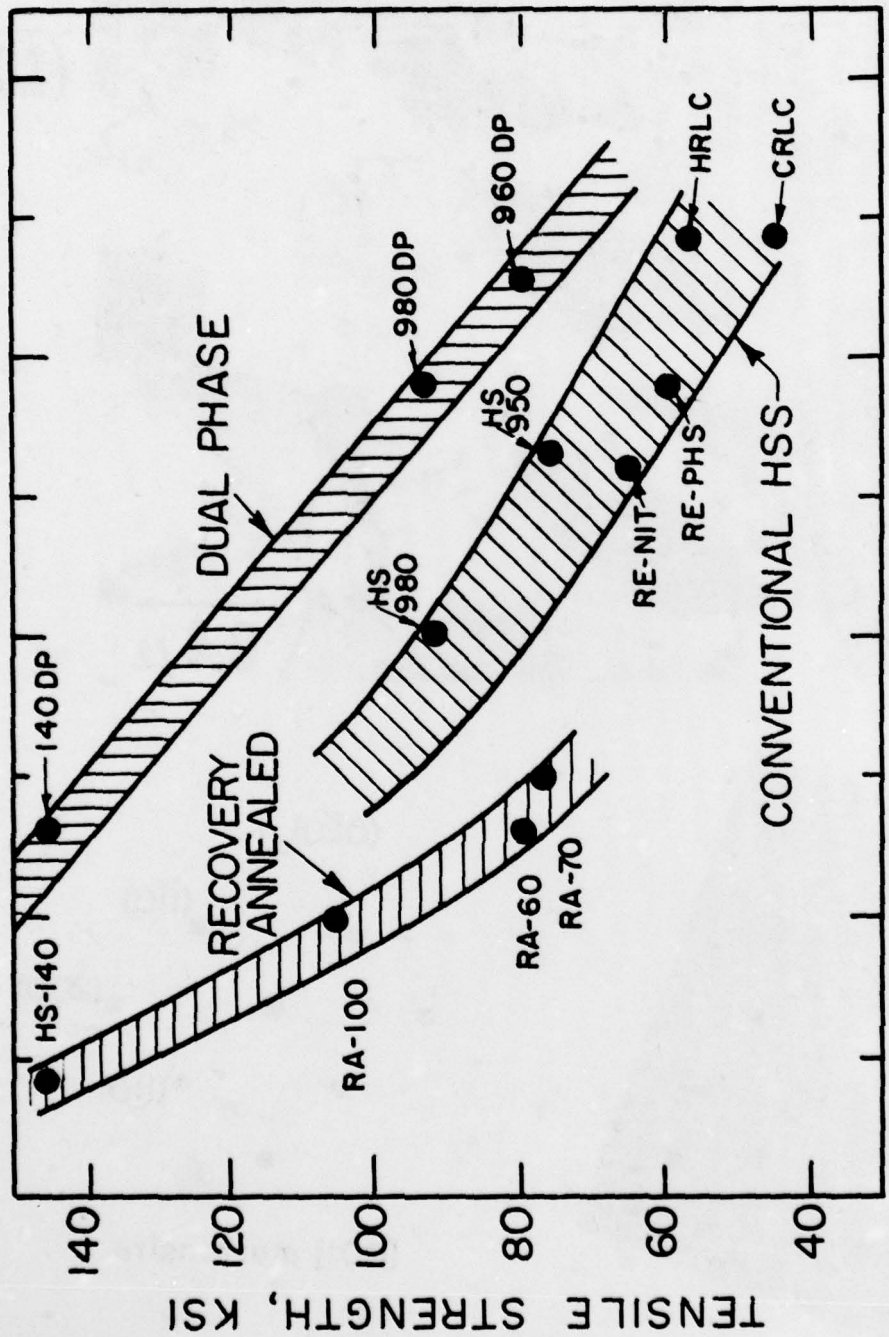

XBL 796-6427

Figure 15

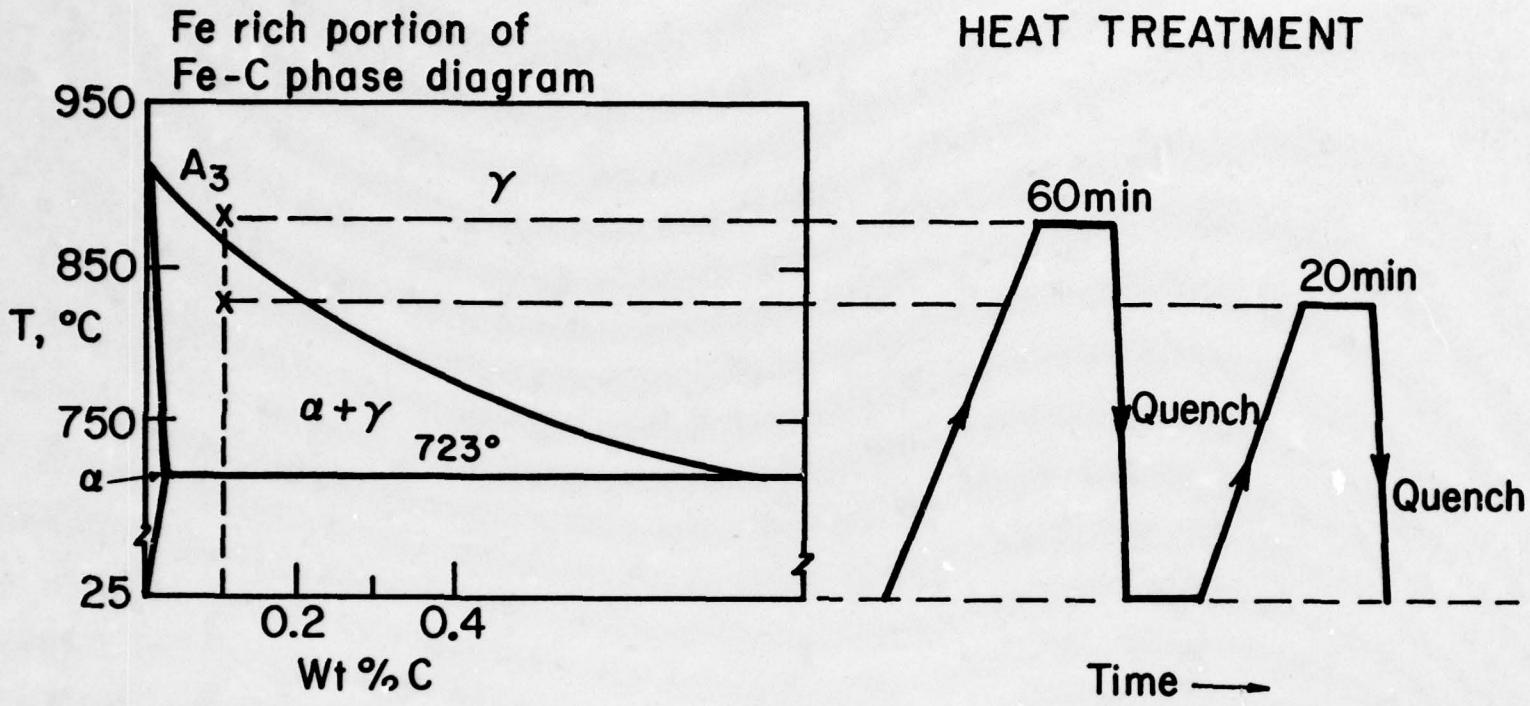

XBL766-9070

Figure 16

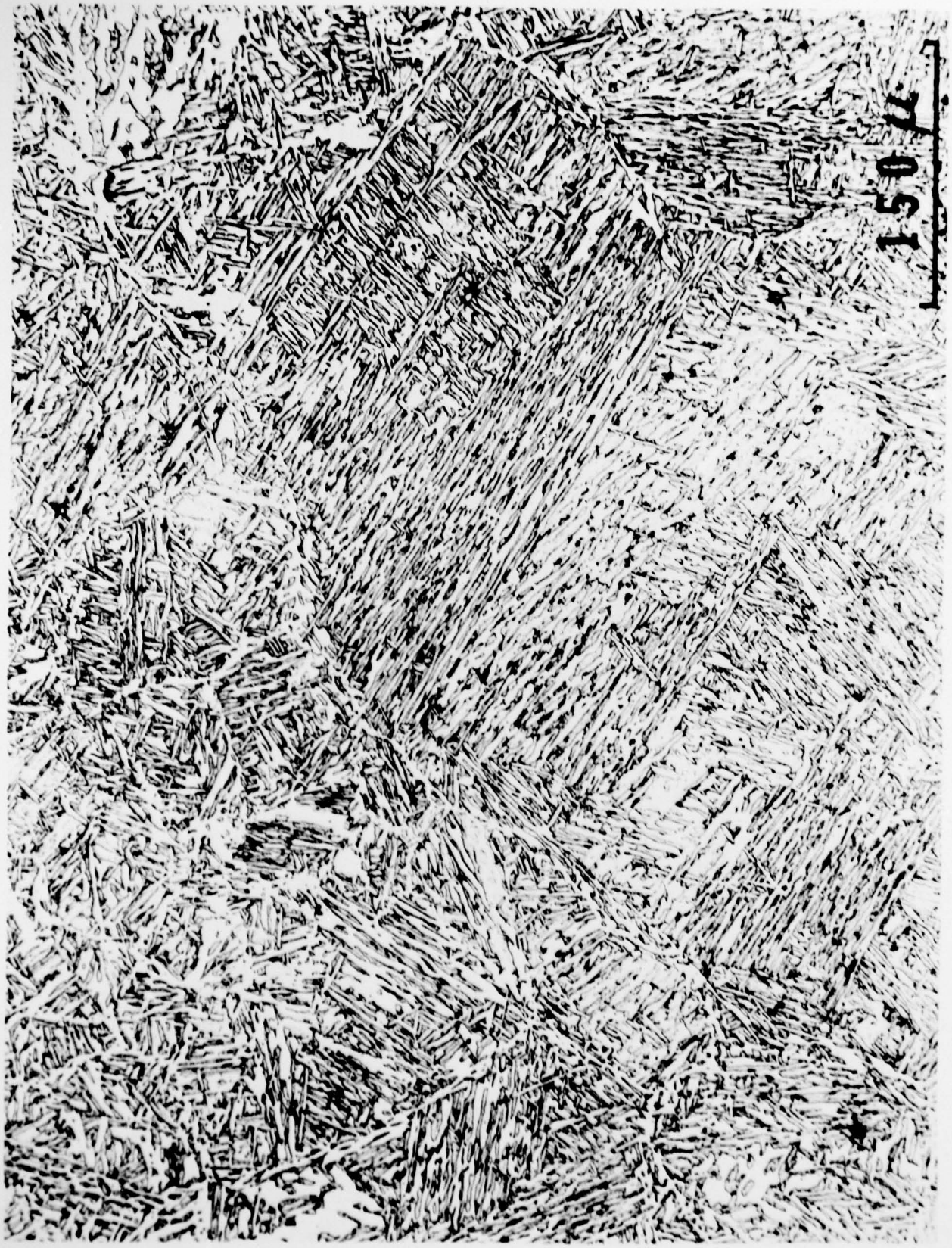

Figure 17

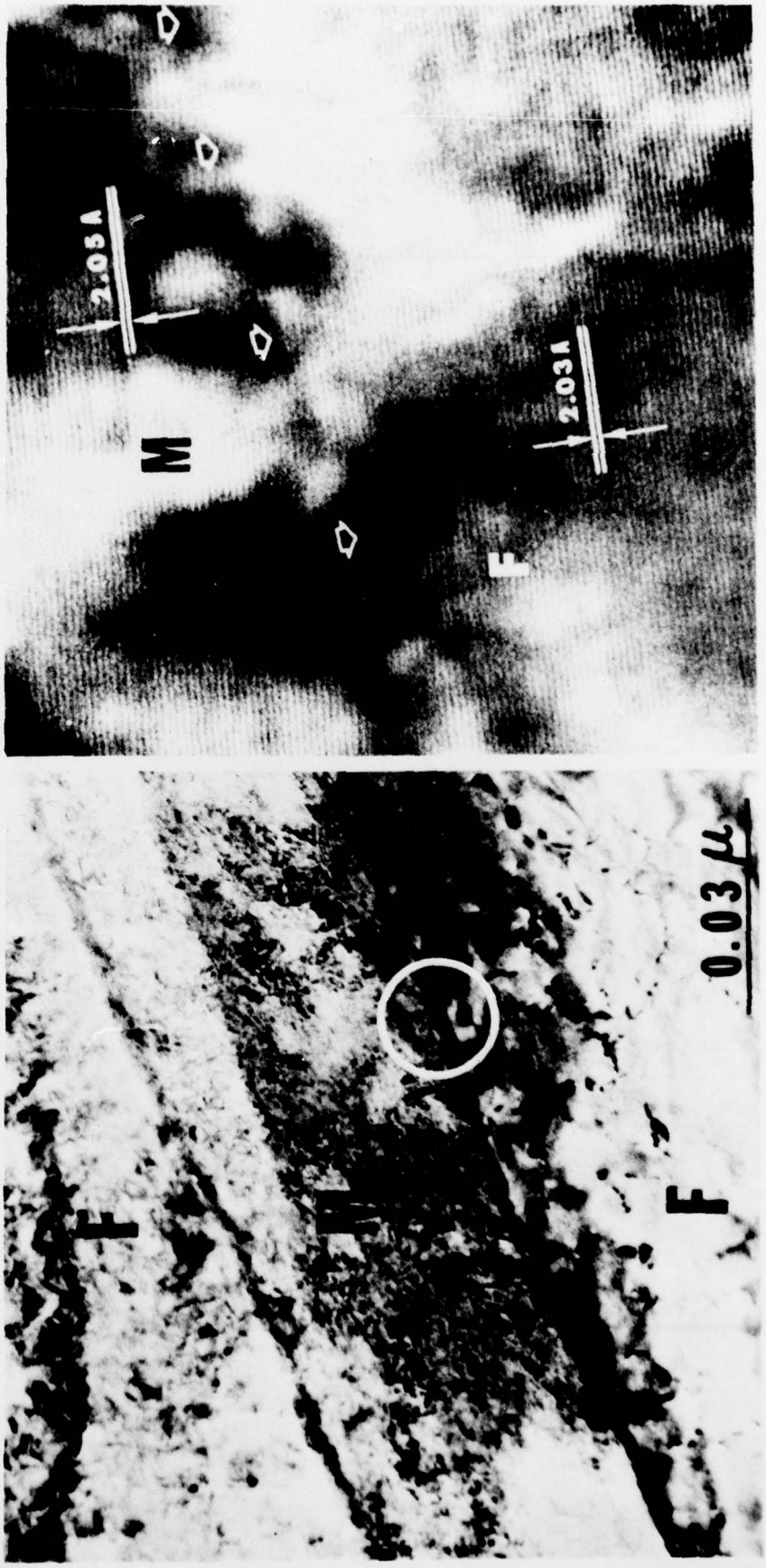

Figure 18

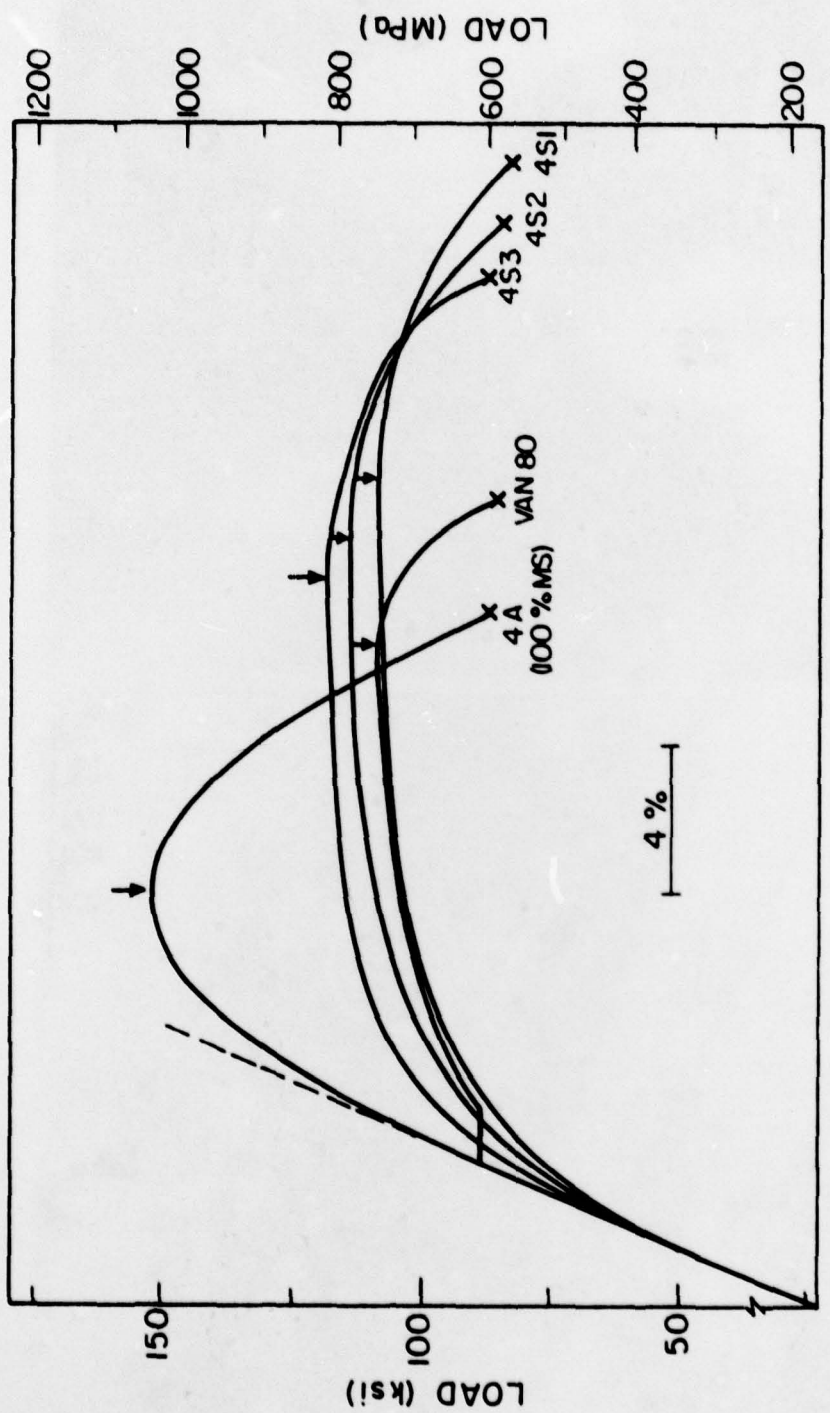

XBL 777-5865

Figure 19

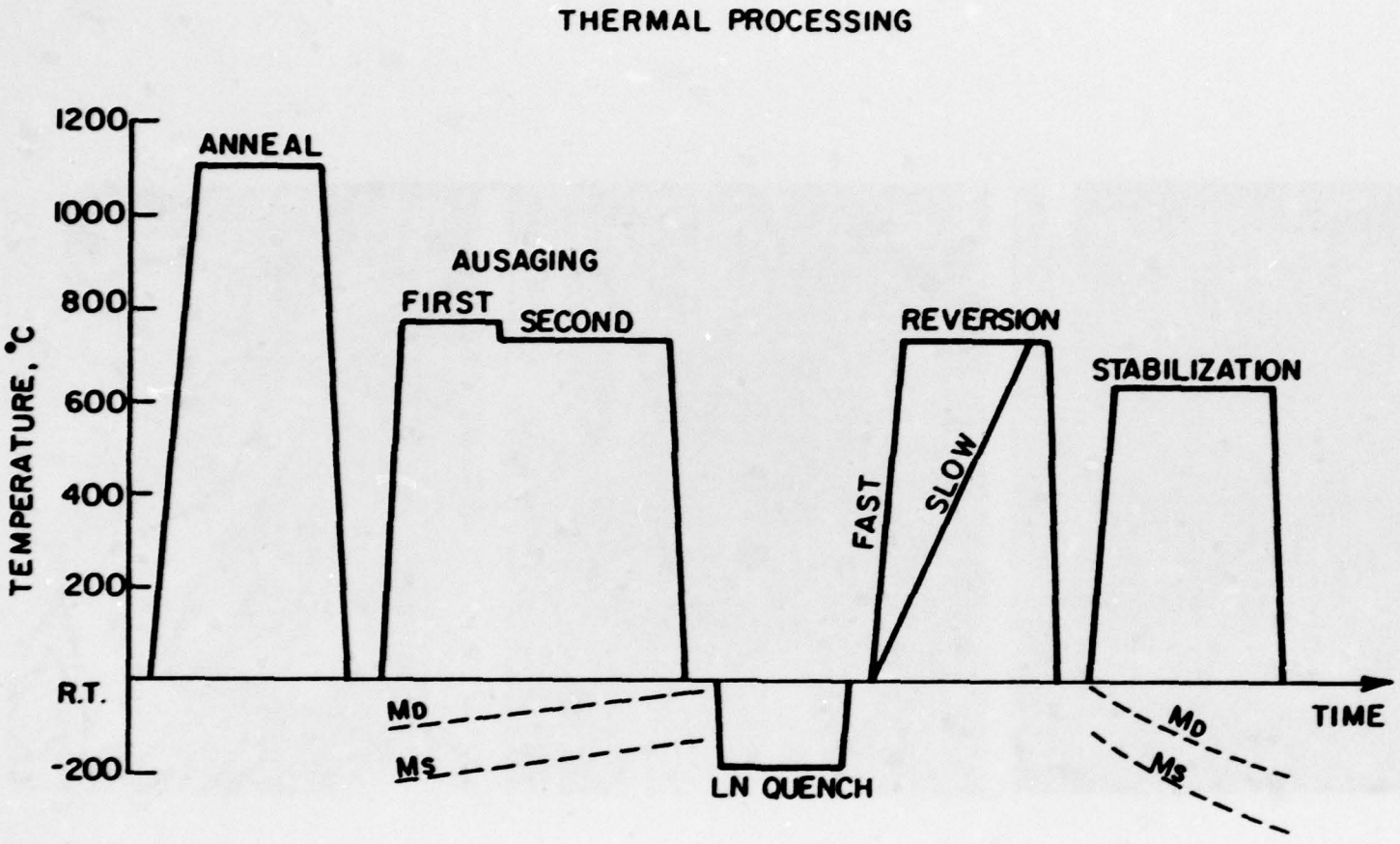

Figure 20

XBL 7710-6283

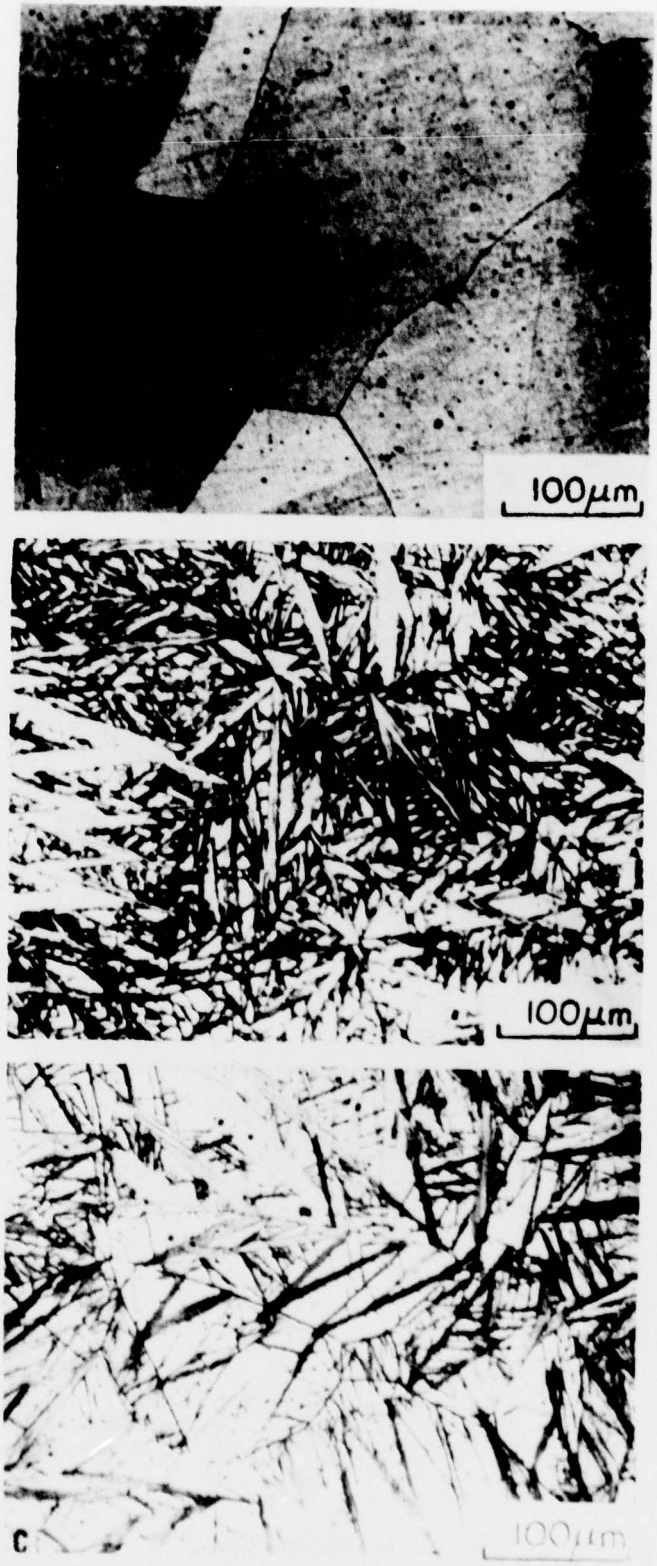

Figure 21

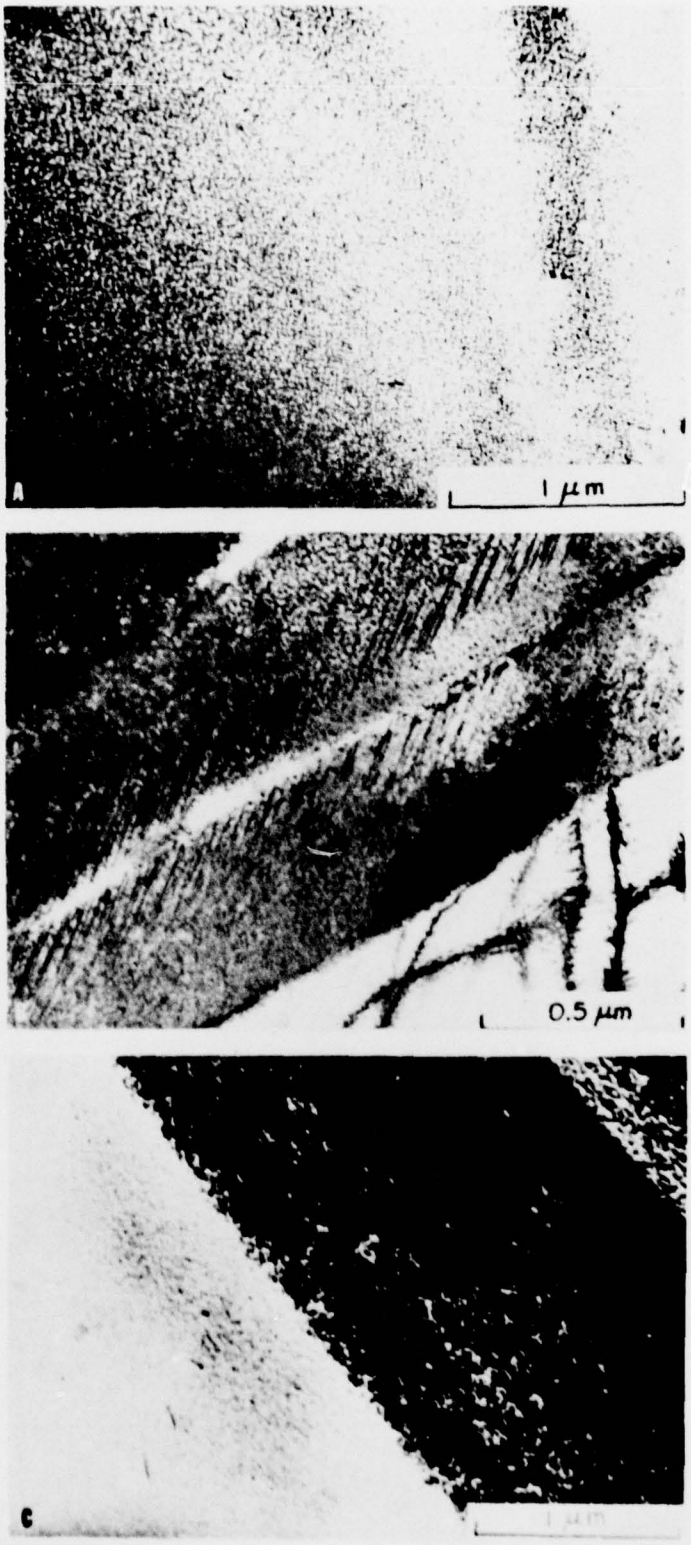

Figure 22

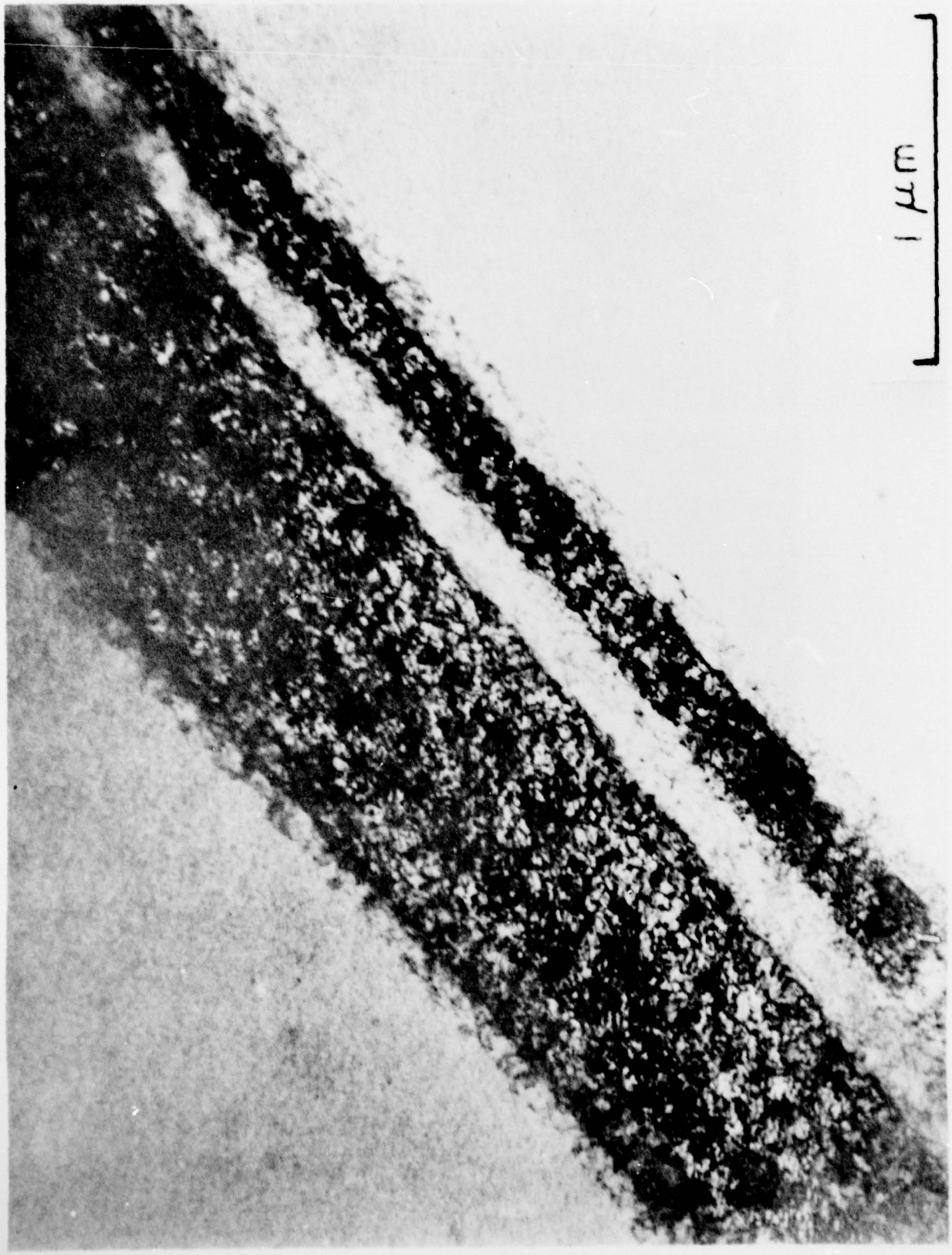

Figure 23

Figure 24

Figure 25

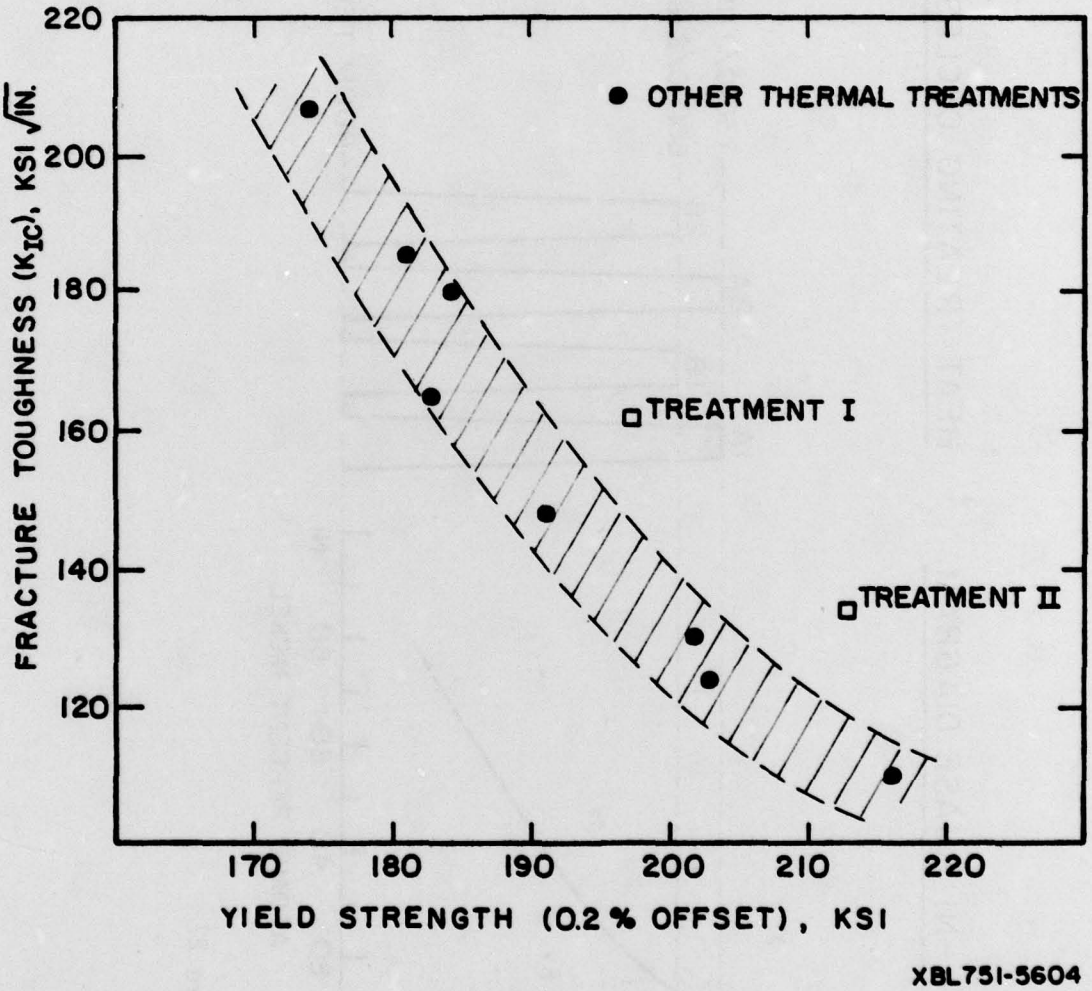
220
200
180
160
140
120
FRACTURE TOUGHNESS (K_{IC}), KSI $\sqrt{IN.}$
● OTHER THERMAL TREATMENTS
□ TREATMENT I
□ TREATMENT II
170
180
190
200
210
220
YIELD STRENGTH (0.2 % OFFSET), KSI
XBL751-5604

Figure 26

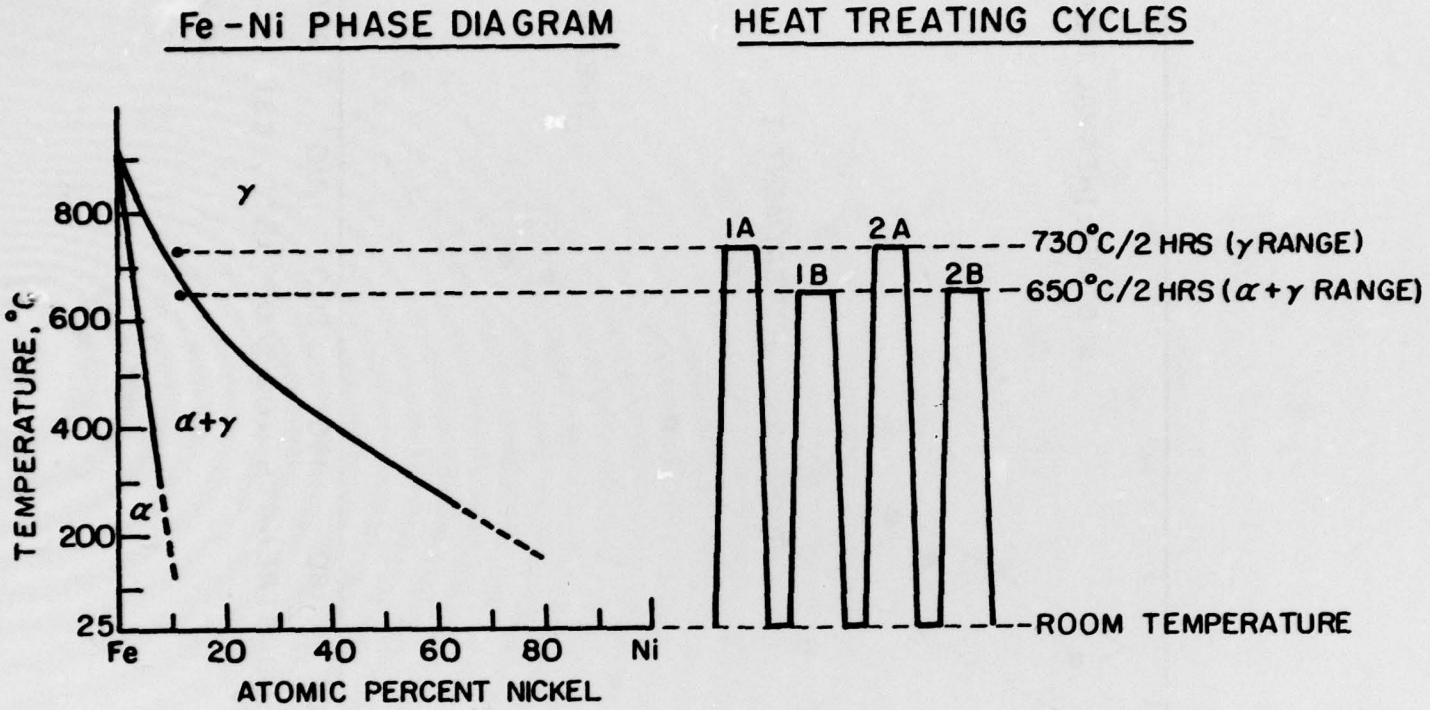
Fe-Ni PHASE DIAGRAM
HEAT TREATING CYCLES
γ
α+γ
α
800
600
400
200
25
TEMPERATURE, °C
Fe
20
40
60
80
Ni
ATOMIC PERCENT NICKEL
1A
2A
1B
2B
730°C/2 HRS (γ RANGE)
650°C/2 HRS (α+γ RANGE)
ROOM TEMPERATURE
XBL 739-1884

Figure 27